MARIA S.MERIAN-Berichte

Greenland melt water in the western Nordic Seas and the Irminger Sea

Cruise No. MSM85

July 23 – August 13, 2019
St. John's (Canada) – Longyearbyen (Norway)

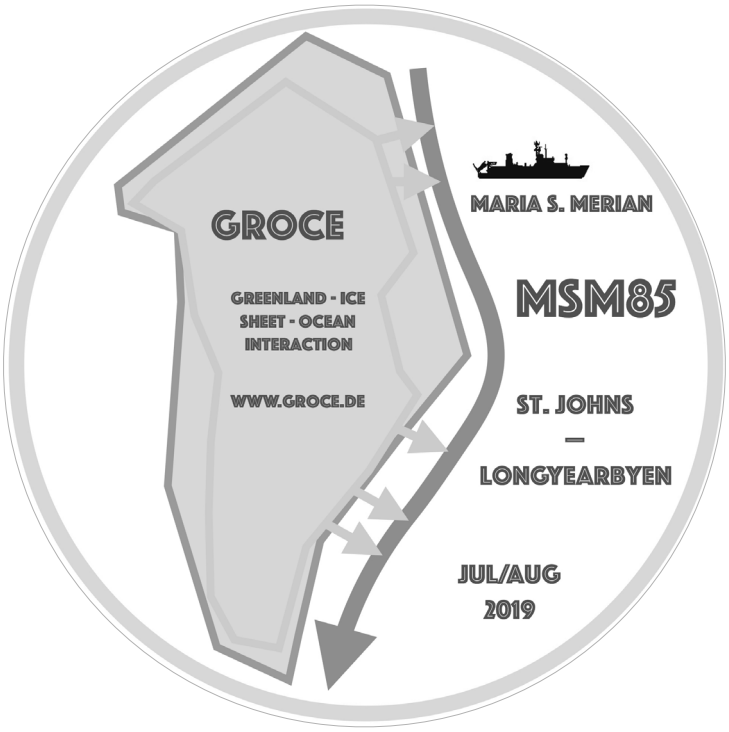

C Mertens, O Huhn, I Rapp, F Benz, J Stiehler, D Bastian, A Filella, K Unger Moreno, J Bornemann, L Böckmann, W Böke, C Chercham, G Fiedler, JR Heinicke, Y Hinse, T Kalvelage, J Kirchner, J Lauber, B Mirau, K Purcel, N Sukhikh

Christian Mertens
University of Bremen

2020

Table of Contents

1 Cruise Summary

1.1 Summary in English

The major goal of the observations on MARIA S. MERIAN cruise MSM85 was to determine the distribution of glacial melt water along the east Greenland shelf and in the East Greenland Current using the noble gases helium and neon as tracers. The trace chemistry group studied the nutrient limitation of phytoplankton growth and how it depends on the ratio of supply of key nutrients to different areas of the ocean. Further a detailed survey of nitrous oxide (N_2O) was carried out as the eastern coast of Greenland is a greatly under-sampled region for this gas. The work program consisted of 160 CTD stations along eight hydrographic sections that were crossing the Greenland Shelf and the East Greenland Current at different latitudes in the Irminger and Greenland Seas. A total of 720 water samples for noble gas analysis were collected and nutrient samples were collected in regular intervals. Underway surface water samples were collected with a trace metal clean surface water sampling device (towfish), which was deployed at 66 locations along the cruise transect for dissolved trace metal samples and other parameters. Underway measurements of dissolved N_2O and CO in seawater were carried out by means of an autonomous equilibrator headspace setup coupled to a trace gas analyzer. The cruise MSM85 was part of the BMBF program GROCE (Greenland Ice Sheet – Ocean Interaction).

1.2 Zusammenfassung

Das Hauptziel der Messungen auf der MARIA S. MERIAN Reise MSM85 war die Verteilung von glazialem Schmelzwasser entlang des Schelfs on Ostgrönland und innerhalb des Ostgrönlandstroms zu bestimmen, wobei die Edelgase Helium und Neon als Tracer des Gletscherschmelzwassers verwendet wurden. Die Gruppe für Spurenchemie untersuchte die Nährstofflimitierung des Phytoplanktonwachstums und wie diese vom Verhältnis der Versorgung verschiedener Regionen mit Schlüsselnährstoffen abhängt. Ferner wurde eine detaillierte Untersuchung von N_2O durchgeführt, da an der Ostküste Grönlands bisher nur wenige Proben vorliegen. Das Arbeitsprogramm bestand aus 160 CTD-Stationen entlang von acht hydrographischen Schnitten in der Irminger- und Grönlandsee, die auf verschiedenen Breiten quer zum Grönlandschelf und zum Ostgrönlandstrom verliefen. Insgesamt wurden 720 Wasserproben für die Edelgasanalyse gesammelt und in regelmäßigen Abständen Nährstoffproben entnommen. Während der Fahrt wurden mit einem Schleppfisch 66 Oberflächenwasserbeprobungen zur Messung von Spurenmetallen durchgeführt. Weiterhin wurden im Dauerbetrieb Messungen von gelöstem N_2O und CO im Meerwasser durchgeführt. Dafür wurde Wasser mit einer In-situ-Pumpe im Seeschacht in einen Spurengasanalysator geleitet. Die Fahrt MSM85 war Teil des BMBF-Programms GROCE (Greenland Ice Sheet – Ocean Interactions).

2 Participants

2.1 Scientific Party

Name	Discipline	Institution
Mertens, Christian, Dr.	Chief Scientist	IUPHB
Böke, Wolfgang	Technician	IUPHB
Huhn, Oliver, Dr.	Noble Gases and Tracers	IUPHB
Bornemann, Julian	Noble Gases and Tracers	IUPHB
Hinse, Yannik	Noble Gases and Tracers	IUPHB
Sukhikh, Natalia	Noble Gases and Tracers	IUPHB
Stiehler, Jan	ADCP	IUPHB
Rapp, Insa, Dr.	Trace Chemistry	GEOMAR
Purcel, Karl	Trace Chemistry	UQAM
Filella, Alba	Trace Chemistry	GEOMAR
Bastian, Daniel	Nitrous Oxide	GEOMAR
Böckmann, Lea	Oxygen	IUPHB
Benz, Frederike	CTD and Oxygen	UHH
Unger Moreno, Katharina	CTD and Bathymetry	IUPHB
Chercham, Carolyne	CTD	UHH
Fiedler, Gregor	CTD	UHH
Kirchner, Julia	CTD	UOL
Lauber, Julius	CTD	UHH
Mirau, Bastian	CTD	IUPHB
Kalvelage, Tim	Journalist	RS
Heinicke, Jan Richard	Photographer	HHAN

2.2 Participating Institutions

IUPHB	Institut für Umweltphysik, Universität Bremen
GEOMAR	Helmholtz-Zentrum für Ozeanforschung Kiel
UHH	Institut für Meereskunde, Universität Hamburg
UQAM	L'Université du Québec à Montréal
UOL	Carl von Ossietzky Universität Oldenburg
RS	Die Reportageschule, Reutlingen
HHAN	Hochschule Hannover

3 Research Program

Melting of the Greenland Ice Sheet (GrIS) is one of the main sources for the global sea level rise. The accelerated melting in the last two decades is mainly attributed to the inflow of warmer water into the fjords of the outlet glaciers. Rates of surface and basal melting are not sufficiently known, also it is unclear how much of the melt water leaves the fjords and enters the East Greenland Current or the interior of the western Nordic Seas.

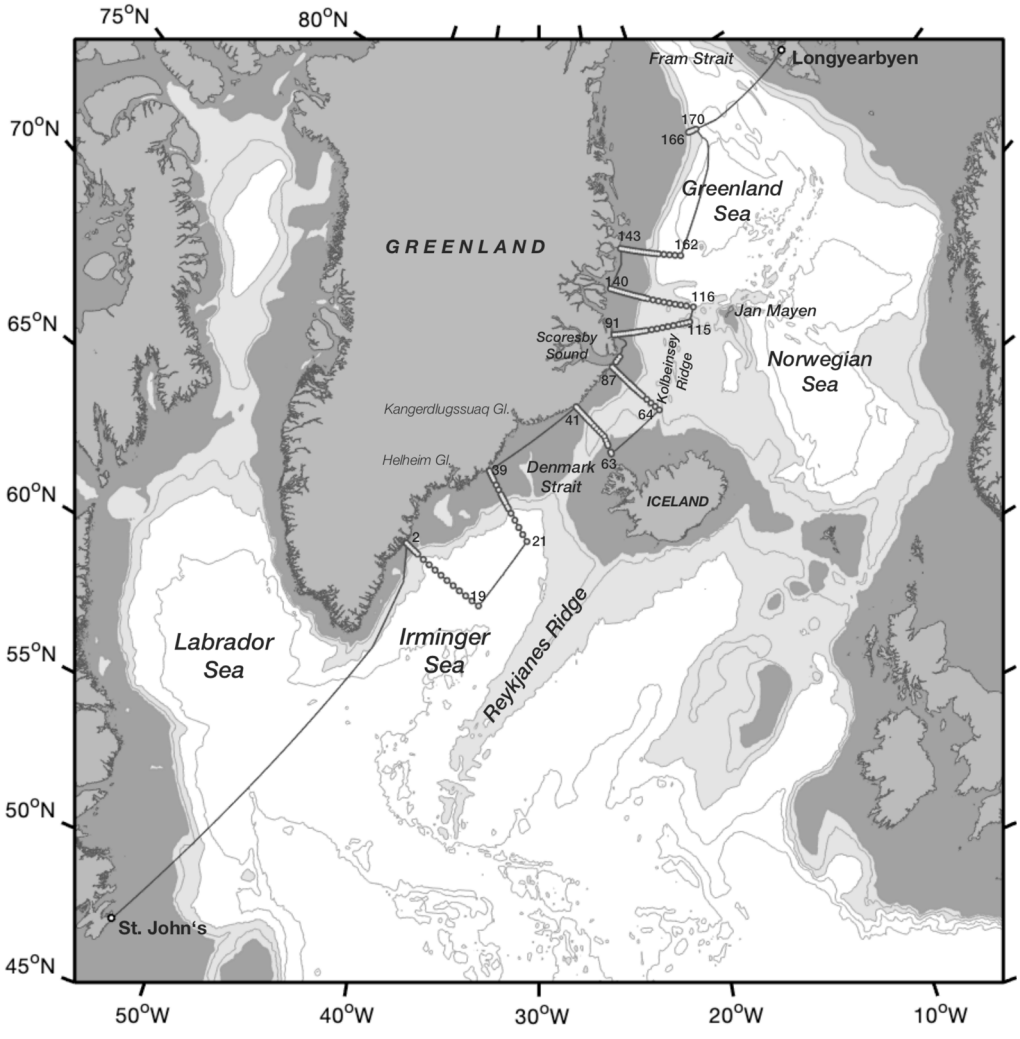

Fig. 3.1 Cruise track and hydrographic stations of MARIA S. MERIAN cruise MSM85 from St. John's (Newfoundland) to Longyearbyen (Svalbard), labels indicate station numbers.

During the cruise MSM85 water samples were collected for helium and neon isotope analysis along eight hydrographic sections across the shelf of East Greenland and across the East Greenland Current. Helium and neon are uniquely suited as tracers of glacial meltwater in the ocean. Parallel sampling of transient tracers (CFCs, SF_6) provide an estimate of the ventilation time and an integral melting rate when combined with the melt water fractions. This distribution of melt water is of more than local interest. The additional freshwater in the key regions of the formation of North Atlantic Deep Water could alter the vertical density stratification, modify the amount of deep water formed, and have consequences for the strength of the climate relevant Atlantic meridional overturning circulation (AMOC). The cruise was part of the BMBF program GROCE (Greenland Ice Sheet – Ocean Interaction, www.groce.de).

The objective of the trace chemistry group on the cruise was to determine how the ratio of different nutrients (principally organic carbon, NO_3 and Fe) affect the community structure. In the context of the changing Arctic, freshening of the East Greenland shelf region is expected in the coming decades which may increase organic carbon and Fe supply, but decrease summertime NO_3 supply due to enhanced stratification. A key research question is therefore how such shifts in the ratios of nutrient availability will affect primary producers. This was addressed by the deployment of a towfish to collect samples for organic carbon species (DOC, CDOM, FDOM), community structure (flow cytometry), nutrient concentrations (nitrate, phosphate and silicic acid) and micronutrient concentrations (trace elements including Fe, Co and Mn). In addition to the underway sample collection, a number of incubation experiments were performed to test the biological response to different combinations of nutrient spikes.

Underway measurements of dissolved N_2O and CO in seawater were carried out to investigate the air-sea dynamics of N_2O, CH_4 and CO. The goals were to decipher the water column distribution of N_2O and CH_4, and to infer their main formation mechanisms.

4 Narrative of the Cruise

MARIA S. MERIAN left the port of St. John's, Canada on July 23 at 16:00 (local time, LT) with a scientific party of 21 people. Shipboard ADCP and thermosalinography measurements were started shortly after leaving the three-mile zone, at about 16:45 (LT). Also deployed was the tow fish used for trace metal sampling. Data acquisition of the multibeam echo sounder was started von July 24. A test of the CTD/rosette was made in the afternoon of July 24. The instrument was lowered to a depth of 100 m and all bottles were closed.

After a transit of 3.5 days across the Labrador Sea, the ship arrived at the first CTD station in the Irminger Sea on July 27 at 05:30 (LT). The station was located close to the coast of Greenland at a water depth of about 180 m. On the following two days 18 CTD stations were made along a section in southeast direction toward the center of the Irminger Sea. The section was completed on July 29 at 03:00 (LT). The second CTD section started after a transit of 176 nm on July 29 at 19:45 (LT). This section was oriented in northwest direction back to the Greenland coast, 19 CTD stations were made until July 31, 09:45 (LT). The transit along the coast to the third CTD section was 236 nm and took until August 1, 08:00 (LT). This section went across Denmark Strait, 23 CTD stations where made along the track. The forth stations started after a transit of 142 nm on August 3 at 01:30 (LT). This section again crossed the Denmark Strait, now in northwest direction toward Greenland. It was completed on August 4 at 08:15 (LT), after 24 CTD casts.

On the transit to the next section three CTD stations where made across the entrance of Scoresby Sound. In the afternoon of August 4 MARIA S. MERIAN reached the marginal ice zone and the speed needed to be reduced to proceed safely through the ice flows, also the tow fish needed to be recovered. The ship arrived at the first station of section five, that was located close to the coast at a depth of 80 m, on August 4 at 22:30 (LT). Due to the ice situation the original plan had to be changed. Instead of completing the section near Jan Mayen, it was terminated after 24 CTD casts and after a short transit in northward direction the next section was started on August 6 at 18:00 (LT). This new section had 24 CTD casts and went back to the Greenland coast. It was finished on August 8 at 10:30 (LT). After a transit along the coast, section six started on August 8 at 21:30 (LT). 19 CTD casts where made along this section which was completed on August 10 at 11:00 (LT). The transit to the last section at 77° 30' N took about 14 hours, and the ship arrived at the first CTD station of this section on August 11 at 13:00 (LT). The most western station on this section was reached at about 5° 2.4' W at a water depth of about 1150 m. From there on four more CTD stations were made in east direction before the work program ended on August 12 at bout 05:00 (LT). On August 13 at 08:30 (LT) MARIA S. MERIAN arrived in Longyearbyen.

5 Preliminary Results

5.1 CTD Measurements

(Frederike Benz)

5.1.1 System Overview and Data Processing

During the MSM85 cruise a total number of 160 CTD casts were carried out, while crossing the East Greenland Shelf and the East Greenland Current. These stations were organized into eight sections, which covered the Irminger, Iceland and Greenland Sea as well as the Denmark Strait. Three additional stations were carried out across the entrance of the Greenlandic fjord Scoresby Sound.

The CTD (Sea-Bird SBE9 underwater unit with Sea-Bird SBE43 oxygen sensor) measured pressure, temperature, conductivity and dissolved oxygen. Additionally, the CTD was equipped with turbidity and fluorescence sensors that were attached to the frame of the rosette. The first six CTD profiles (stations 2-7) were carried out without the fluorescence sensor. Specific information about the CTD configuration are summarized in Table 5.1.

The rosette was carrying 22 Niskin bottles with a volume of 10 l and two ADCPs (upward- and downward looking). To determine the distance between the rosette and the sea floor, an altimeter with a range of about 70 m was installed. A CTD deck unit, which is a computer system for data logging and closing of the Niskin bottles, plus a GPS were installed as well. The data were recorded and processed by using the Seasoft software.

The regular procedure during a CTD cast was to lower the CTD to a water depth of 10 m. After the pump started, the CTD was heaved to the surface and directly afterwards lowered to a water depth of at least 10 m above the bottom was reached (the distance to the bottom varied, depending on the sampling). After that, the CTD rosette was heaved again to a water depth of 10 m. On the way up, the Niskin bottles were closed in various depths. However, in bad weather situations, the CTD profile procedure was a bit different. Then the CTD was lowered to a water depth of 20 m at the beginning of the profile and after the pump started the CTD was heaved to

10 m. At the end of the profile the CTD was heaved again to a water depth of 20 m. The *bad weather* CTD profile procedure was carried out for the stations 31-39.

Table 5.1 Summary of CTD system configuration used during MSM85.

Sensor	Model	Serial Number	Channel
Temperature	Sea-Bird SBE9	4156	1. Frequency
Conductivity	Sea-Bird SBE9	2646	2. Frequency
Pressure	Digiquartz with TC	0657	3. Frequency
Oxygen	Sea-Bird SBE43	0267	V0
Altimeter		75743	V2
Flurometer[1]	WET labs, ECO-AFL/FL	1754	V4
Turbidity Meter	WET labs, ECO-NTU	1754	V5
Turbidity Meter	Seapoint	12345	V6

[1]no flurometer data on stations 2-7

After the CTD cast was finished, water samples were taken from the Niskin bottles. Salinity and oxygen (O_2) samples were taken for calibration purposes. Salinity samples were taken from the Niskin bottles at 13 stations and will be analyzed in the lab in Bremen. O_2 samples were taken from the Niskin bottles at 79 stations and the calibration was done with the *Winkler titration method* during the cruise. During station 61 the pump of the CTD was blocked. That could be fixed after the station was finished, but due to this reason the recorded data for station 61 could not be used.

5.1.2 CTD Oxygen Sensor Calibration

To calibrate the CTD oxygen sensor, the difference between the O_2 concentration determined by titration and the O_2 concentration measured by the sensor, when the bottles were fired, is calculated (Fig. 5.1). A limit of two standard deviations around the median was calculated and the values outside these limits were not taken into account. In total 40 difference values are neglected. Thus, the higher variability in the difference in water depths ≤ 100 m is corrected.

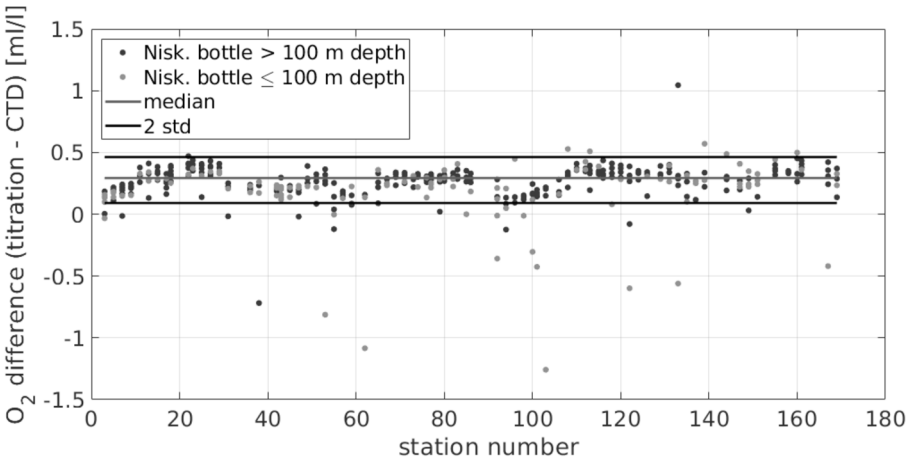

Fig. 5.1 Difference between the CTD O_2 sensor concentration and the O_2 concentration determined by the Winkler titration method (titration - CTD). The median (red) and the two standard deviations (black) are presented as lines. The dots describe the O_2 differences for the Niskin bottles, closed in water depth > 100 m (blue) and ≤ 100 m (green).

Figure 5.1 does not show the dependency of the O_2 differences on pressure, temperature, salinity and O_2, therefore the O_2 differences are plotted against those variables and a linear fit is applied. Figure 5.2 shows a linear dependency of the O_2 difference and pressure (Figure 5.2 (a)). Therefore the O_2 difference values are corrected by subtracting the linear fit. The linear fits in Figure 5.2 (b), (c) and (d) show that the dependency of the O_2 difference and the variables temperature, salinity and O_2 can be neglected. This yields the calibration polynomial:

$$O_{2,calibrated} = O_{2,CTD} + 5.38 \cdot 10^{-5} \cdot P + 0.24$$

where $O_{2,CTD}$ is the O_2 measured by the CTD and P is the pressure. Using all the samples within the two standard deviations for the water depth >100 m an Root Mean Square (RMS) uncertainty of 0.07 ml/l is determined.

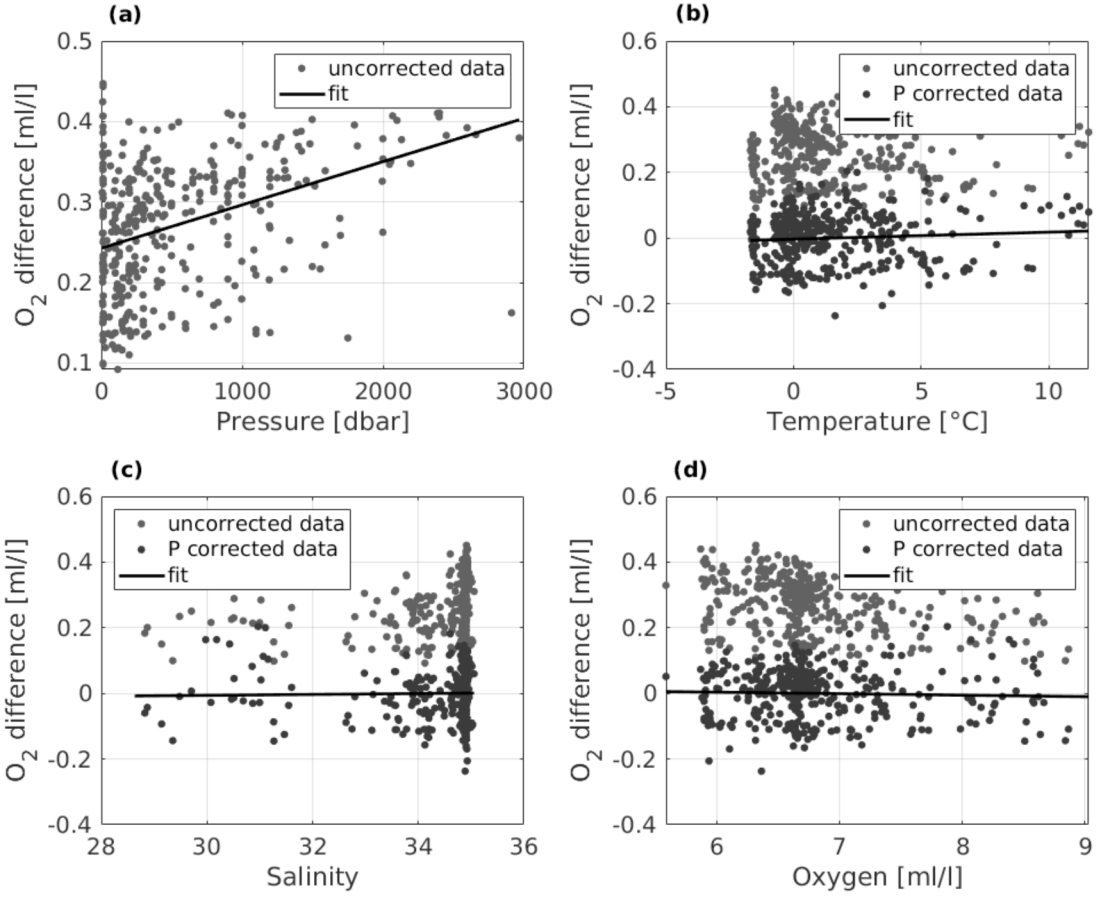

Fig. 5.2 Fitting and correction of the O_2 difference (O_2 titration - O_2 CTD) against pressure, temperature, salinity and oxygen, measured by the CTD. The red dots represent the uncorrected data and the blue dots reprensent the data, where the drift of the pressure is corrected. The linear fit is represented as black line.

5.1.3 CTD Sections

The CTD measurements carried out during the MSM85 cruise can be separated into eight sections. Section 1 and 2 are located in the Irminger Sea, section 3 is situated in the entrance of the Denmark Strait and the sections 4-8 are located in the Greenland Sea. One additional section is located across the mouth of Scoresby Sound.

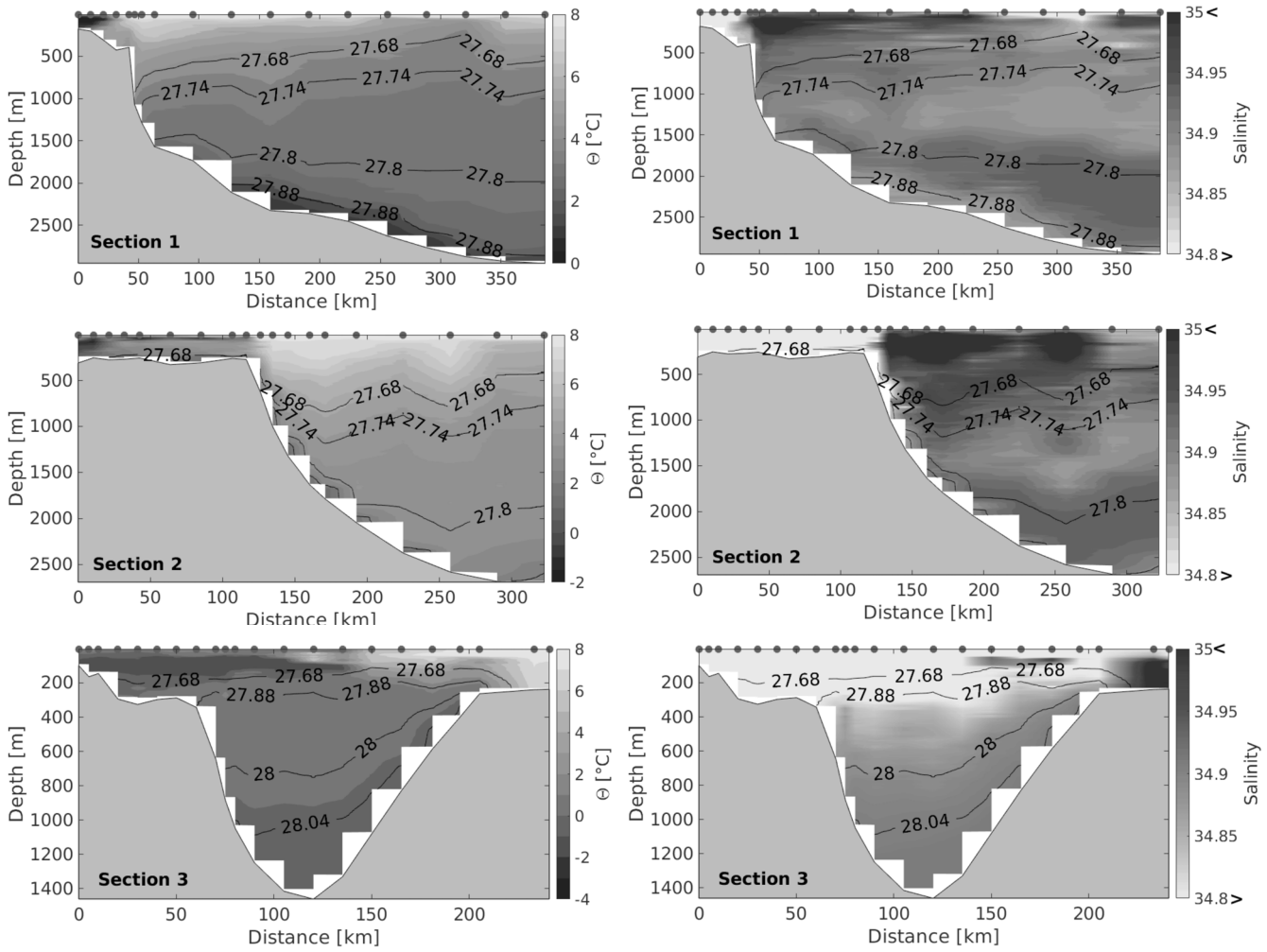

Fig 5.3 Vertical sections of potential temperature (Θ) (left) and salinity (right) with contours of potential density (kg/m³) for the sections 1, 2 and 3. The locations of the sections are shown in Fig. 3.1. The red dots indicate the positions of the CTD profiles. Note that the range of the colorbars are different.

Figure 5.3 shows preliminary visualisations of the sections 1, 2 and 3. Section 1 and 2 (Irminger Sea) show a hydrographic front situated on the edge of the Greenland continental shelf. On the western side of the front there is relatively fresh and cold water (Θ = 0 °C and S =< 34.8 for section 1 and Θ = -1.3 °C at the coldest spot and S =< 34.8 for section 2), which could be transported by the East Greenland Current (EGC). On the eastern side of the front there is rather warm and salty water, especially in the upper layer (Θ = ~7 °C and S = > 35 for section 1 and Θ = ~7 °C and S = > 35 for section 2), which might be transported by the Irminger Current (IC). For section 1 and 2, the water mass in the intermediate layer east of the front, can be associated with Labrador Sea Water (LSW) (Θ = 3.3 °C and S = 34.87 for section 1 and Θ = 3.4 °C and S = 34.87 for section 2). On the Greenlandic slope a dense plume ($\rho \geq 27.8$ kg/m³) can be identified as well which could be associated with the Denmark Strait Overflow (DSO). Section 3 was carried out further north in the entrance of the Denmark Strait. The upper layer is mainly dominated by cold and fresh water (Θ = -1.6 °C at the coldest spot and S = < 34.8), which is probably transported by the EGC as well. The Iceland continental shelf (eastern of the section) is dominated by warm and salty water (Θ = ~7 °C and S = > 35), which is probably transported by the northward flowing IC.

5.2 Oxygen Sampling

(Frederike Benz)

Oxygen samples were taken from the Niskin bottles at almost every second station. The O_2 concentration was determined using the Winkler titration method. After the sampling the bottles were stored in the dark for at least one hour and the titration was performed within 12 hours. A total number of 493 samples were taken from 77 CTD stations, while 74 double samples were taken to determine the quality of the sampling and titration procedure. At the end, 6 samples were not taken into account for the analysis, because they were marked as bad data due to swapped lids or mistakes during the sampling or titration procedure.

The Niskin bottles from which the O_2 samples were taken were always closed in water depths of 10 m and 10 m above the bottom as well as in depths where the profiles showed very small to no vertical gradient in O_2 concentration. O_2 was always sampled (~6 samples per O_2 station) before any other samples were taken from the bottles, to avoid contamination with atmospheric O_2. For the sampling procedure the O_2 flasks and lids were rinsed with the seawater from the Niskin bottles. Then a silicone hose, which was connected with a Niskin bottle, was inserted until the bottom of the flask where the flasks were rinsed with the overflowing seawater for approximetaly two times of the volume of the flask. During this procedure, the flasks were rotated to make sure that no air bubbles remain in the flask. While pulling out the hose of the flask the hose was squeezed, so that less water was flowing while filling the flask all the way up to the edge. To fix the O_2, 1 ml of alkaline solution (NaOH+KI) and 1 ml of of manganese(II)-chloride ($MnCl_2$) were added to the samples directly after the sampling, which were then shaken (~30 seconds) until all the dissolved O_2 was bounded. After the sampling the O_2 flasks were stored in the dark until the beginning of the titration procedure.

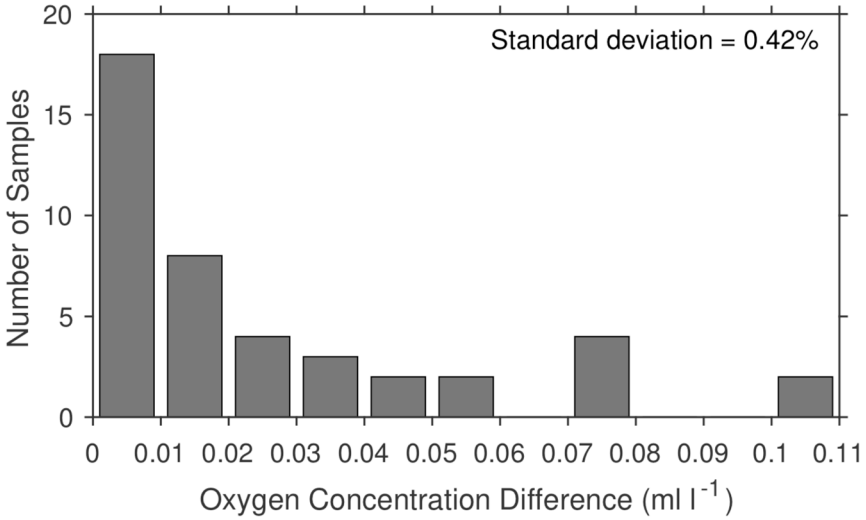

Fig. 5.4 Histogram of the differences between the O_2 double samples.

The first step of the titration procedure was to add 1 ml of 50% sulfuric acid (H_2SO_4) to the samples. Then the Schott TitroLine alpha system was used to determine the dissolved O_2 in the samples. The samples were measured directly in the sampling flask. The Schott TitroLine alpha system uses the Winkler titration method and determines the O_2 concentration in the samples through the amount of titer (thiosulfate, $Na_2S_2O_3$), which is necessary to add, to achieve the endpoint (amount of $Na_2S_2O_3$ to balance the winkler relation). Moreover, a titer test as a

standardization procedure to determine a correction factor was carried out every day on which the titration procedure was performed and always when a new $Na_2S_2O_3$ solution was prepared. For the titer test, 1 ml KIO_3, 1 ml H_2SO_4, and 5 ml KI (in this order) were dissolved in 200 ml distilled water. With this solution the titration procedure was performed. To determine the correction factor, the titer test procedure was repeated three times, while the mean of those delivered the correction factor. To determine the accuracy of the titration procedure, at the end 71 double samples are analyzed (Figure 5.4). The individual double samples are presented in the histogram, which shows a standard distribution around the mean of -0.006 ml/l and a standard deviation of 0.09 ml/l.

5.3 Sampling of Noble Gases (He, Ne) and Transient Tracers (CFC-12, SF6)

(Oliver Huhn)

The Greenland Ice Sheet (GrIS) faces accelerated melting due to Global Warming. This melting happens by surface melting, iceberg calving, as well as by submarine melting, where the ice masses flowing down Greenland get in contact with the warming ocean. This submarine melt water (SMW) contributes to sea level rise and to addition of fresh water into the ocean. If this additional freshwater is transferred by the East Greenland Current or the deep circulation into the Labrador Sea, it might reduce the formation of Labrador Sea Water due to its lower density.

Estimates of submarine melt rates are usually based on indirect methods (difference between total mass loss from remote sensing methods and surface mass balance or estimated from measurements of ice velocities and ice thickness changes) and are still uncertain. So far, there are no sufficient data available that might allow to trace the pathways of GrIS submarine meltwater and to quantify its inventories off their sources in the ocean.

The major aim of the oceanic helium (He) and neon (Ne) sampling during this expedition is to quantify the amount of submarine melted glacial ice and its oceanic pathways of discharge along the East Greenland coast, along the shelf and slope. He and Ne directly infer the amount of SMW. The transient tracer (CFC-12 and SF_6) sampling will help to assess the transit time (or "ages") of the carrying water masses and, hence, the formation and transport rates of SMW.

5.3.1 Approach and Methods

The oceanic measurement of the low-solubility and stable noble gases helium (He) and neon (Ne) provide a useful tool to identify and to quantify submarine melt water (e.g. Schlosser et al. 1986; Huhn et al., 2008; Huhn et al., 2018; Rhein et al, 2018). Atmospheric air with a constant composition of these noble gases is trapped in the ice matrix during formation of the meteoric ice. Due to the enhanced hydrostatic pressure at depth or at the ice shelf base inside an ice shelf cavity, these gases are completely dissolved in the water, when the ice is melting. This leads to an excess of Δ4He = 1280% and ΔNe = 890% in pure SMW (Loose & Jenkins, 2015; the Δ stands for the noble gas excess over the air-water solubility equilibrium). Surface meltwater would equilibrate quickly with the atmosphere and does not lead to any noble gas excess in the ocean water. With an accuracy of <0.5% for He measurements performed at the IUP Bremen, SMW fractions of <0.05% are detectable.

Whereas the total concentration of He and Ne directly allows to calculate the amount of SMW (e.g. Rhein et al., 2018), the He/Ne ratio permits inference of previous sea ice formation (brine

rejection) and melting, by which He and Ne atoms are incorporated into sea ice or rejected in slightly different ratios (Hahm et al., 2004). To regard this effect, the isotopic ratio $^3He/^4He$ is a useful cross-check, but which might be altered by addition of ^3He from tritium decay (tritium was introduced into the atmosphere and (via precipitation) into the ocean from hydrogen bomb tests in the 1950th and 1960th). To estimate the tritiogenic ^3He we additionally sample for tritium.

The anthropogenic transient trace gases chlorofluorocarbon (CFC-12) and sulfur hexafluoride (SF6) enter the ocean by gas exchange with the atmosphere. Since the evolution of these transient tracers in the ocean interior is determined on first order by their well-known temporal increase in the atmosphere and subsequent inner-oceanic advection, they allow estimating the time scale of the renewal and ventilation (the "age") of inner oceanic water masses from the ocean surface, i.e. their formation and overturning time scales. Combining CFC-12 and SF_6 based transit times with the noble gas based SMW fractions and integrated inventories allow calculating GrIS melt rates and oceanic transport rates.

5.3.2 Work at Sea

In total we took 720 water samples for noble gases (He, Ne) from 77 stations along the 8 sections (see map in Figure 5.5, red circles). The water samples for He and Ne were tapped from the CTD/water bottle system into gas tight copper tubes preventing air bubbles inside the tubes, which were then clamped of at both sides. The noble gas samples will be analyzed later in the IUP Bremen noble gas mass spectrometry lab. There, the copper tube water samples are processed in a first step with an ultra high vacuum gas extraction system. Sample gases are transferred via water vapor into a glass ampoule kept at liquid nitrogen temperature. For analysis of the noble gas isotopes the glass ampoules are connected to a fully automated ultra high vacuum mass spectrometric system equipped with a two-stage cryogenic trap system. The system is regularly calibrated with atmospheric air standards (reproducibility better ±0.2%). Also measurement of blanks and linearity are done. For details see Sültenfuß et al., 2009.

We collected 450 water samples for transient tracers (CFC-12, SF_6) from 49 stations along the 8 sections (see map in Figure 5.5, blue dots). For the transient tracers the water samples from the CTD/water bottle system were collected into 200 ml glass ampoules and were flame sealed after a tracer free headspace of pure nitrogen had been applied. The CFC samples are later analysed in the CFC-laboratory at the IUP Bremen. The determination of tracer concentration will be accomplished by purge and trap sample pre-treatment followed by gas chromatographic (GC) separation on a capillary column and electron capture detection (ECD). The amount of tracer degassing into the headspace will be accounted for during the measurement procedure in the lab. The system will be calibrated by analyzing several different volumes of a known standard gas. Additionally the blank of the system will be analyzed regularly.

Additionally we took 140 water samples for tritium on 17 stations on the first 7 sections (see map in Figure 5.5, black circles). The water samples were collected from the CTD/water bottle system and were stored in 500 ml plastic bottles with a water vapour tight plastic lid. All samples were shipped home for later analysis. In a first step the water samples are to be de-gassed with an ultra-high vacuum gas extraction system and will be stored in flame sealed glass containers for the so called helium ingrowth method. During the storage time of several months, part of the 3-H will decay to 3-He by β^- decay. After the storage and a sufficient amount of 3-He ingrowth the water samples will be processed in a second step with an ultra-high vacuum gas extraction

system. The extracted gases containing 3-He from tritium decay are transferred via water vapor into a glass ampoule kept at liquid nitrogen temperature. For analysis of the 3-He the glass ampoules are connected to a fully automated ultra-high vacuum mass spectrometric system equipped with a two-stage cryogenic trap system. The system is regularly calibrated with atmospheric air standards (reproducibility better ±0.2%). Also measurement of blanks and linearity are done. For further details of the method see Sültenfuß et al., 2009. By the known decay time of tritium and the known storage time, the measured 3-He can be converted to the 3-H content in the sample.

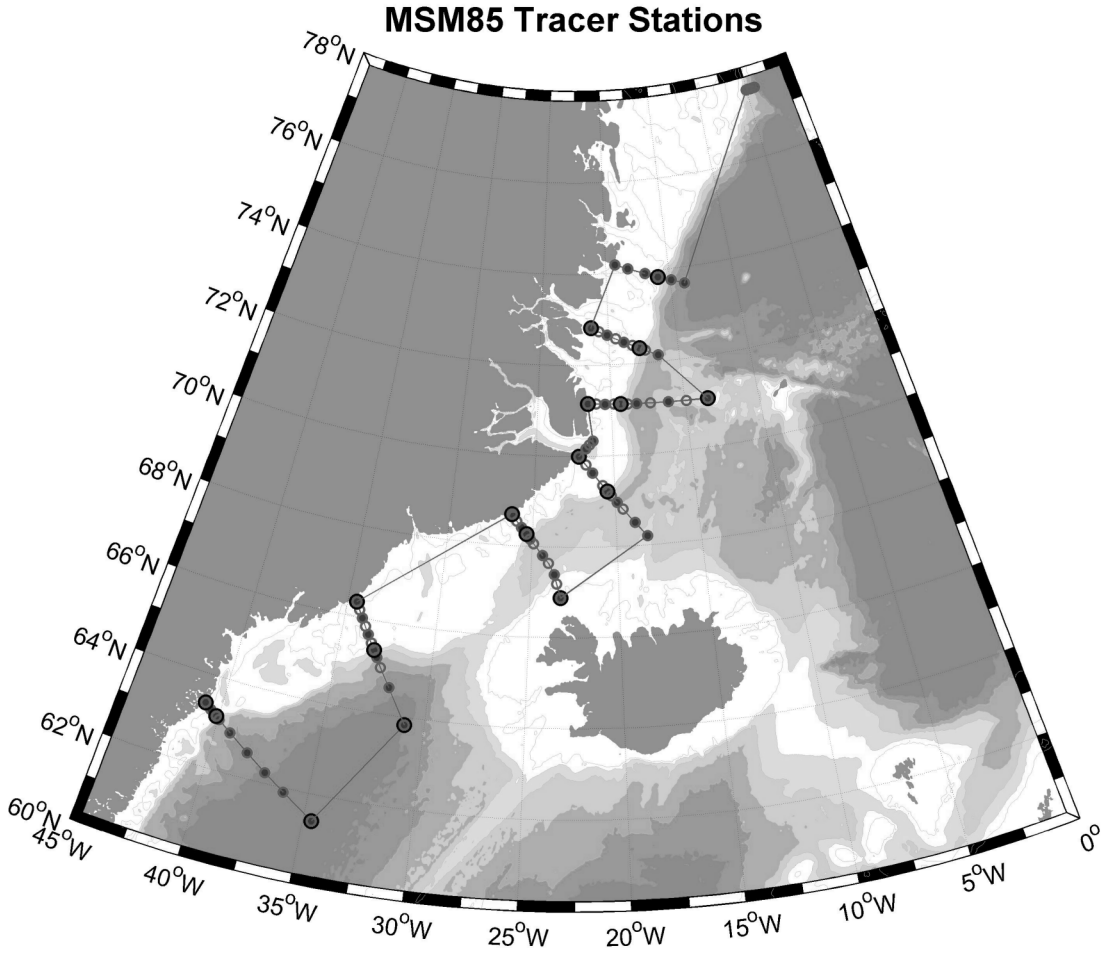

Fig. 5.5 Map of the area of investigation during Maria S. Merian expedition MSM85. The red line is the cruise track. The red circles show locations of stations along the sections with He and Ne sampling. Blue dots indicate stations with CFC-12 and SF6 samples. The black circles indicate stations with additional tritium sampling. White to blue colored is the bathymetry in 1000 m steps.

All samples will be shipped home after the expedition and will be analyzed in the UHB-IUP noble gas laboratory HELIS. The noble gas and transient tracer measurements are expected to be completed one year after arrival in our home lab in Bremen. A careful data quality check will be carried out then.

5.4 ADCP Measurements

(Jan Stiehler)

5.4.1 Shipboard ADCP

Two shipboard acoustic Doppler current profilers (SADCPs), a 75 kHz and a 38 kHz Ocean Surveyor (OS) by Teledyne RD Instruments (TRDI), were installed in the ships hull and were used simultaneously to continuously measure the current velocities in the water colum below the ship. The covered depth was 600m (1300m) for the OS75 (OS38) with a bin length of 8m (32m). Both devices were used in the narrowband mode to provide a maximum vertical range. The OS75 is permanently mounted into the ships bow while the OS38 was installed in the sea chest. Because the SADCPs do not have any build in tilt sensors, the ships GPS position and attitude were obtained from the Seapath system. All data was collected using TRDIs VmDas software, version 1.49. Data recording was started on 23 July 2019 19:14 UTC east of Newfoundland and finished on 12 August 2019 11:00 UTC between Greenland and Svalbard. All systems worked without any problems and the data recording was restarted approximately every 24 hours for a better readability of the data.

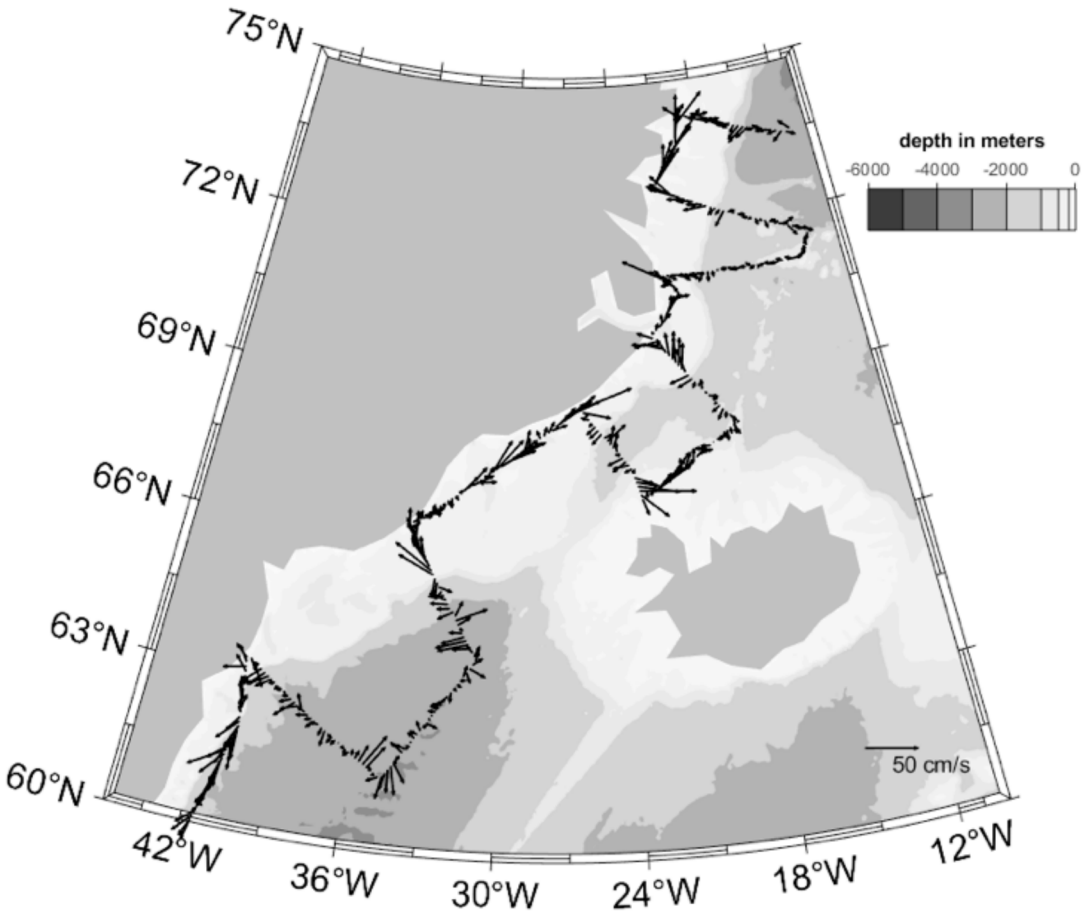

Fig. 5.6 Mean velocity in the depth range of 40m to 480m from shipboard ADCP measurements.

The data wer processed during the cruise using the VMADCP-toolbox OSSI v1.9 for MATLAB of the GEOMAR Helmholtz Centre for Ocean Research Kiel. To determine the actual water depth the bathymetry data taken during the cruise were used. During the processing a water-track calibration was performed to determine phase and amplitude of the transducer

missalignment. This was done by minimizing the root-mean-square differences between estimated water velocities over the ground before and after the ship accelerated. The determined missalignment was -47.2015° (0.3664°) with an amplitude factor of 1.0075 (1) for the OS75 (38). The final results have a temporal resolution of 1 minute and contain zonal and meridional velocities, distributed over latitude, longitude, depth and time along the track of the ship.

The instruments worked properly during the cruise and didn't had any problems. After the first deployment (#000) the configuration was changed to a preset missalignment angle of 0° instead of -45° for the OS75. The data quality is good due to relatively stable weather conditions, except on 30 August 2019 where strong winds were encountered. However the processed data need additional steps of quality control, e.g. detailed inspection and manual removal of suspicious sections close to the surface and the seafloor.

5.4.2 Lowered ADCP

Two Teledyne RD Instruments 300 kHz Workhorse Monitor ADCPs were atached to the CTD-rosette and used in a synchronized configuration, in which the downward looking ADCP (SN 7915) triggered the upward looking ADCP (SN 2161). The intruments were used with a ping rate of 1 Hz and 10 m depth cells. Power was supplied by a single modified Aanderaa pressure housing with 35 commercial 1.5 V batteries. The rosette was lowered and heaved with 1.0 m/s except 100 m closest to the surface and the seafloor, were a speed of 0.5 m/s was used for heaving and lowering. For the exact depth Information the CTD presure data was used.

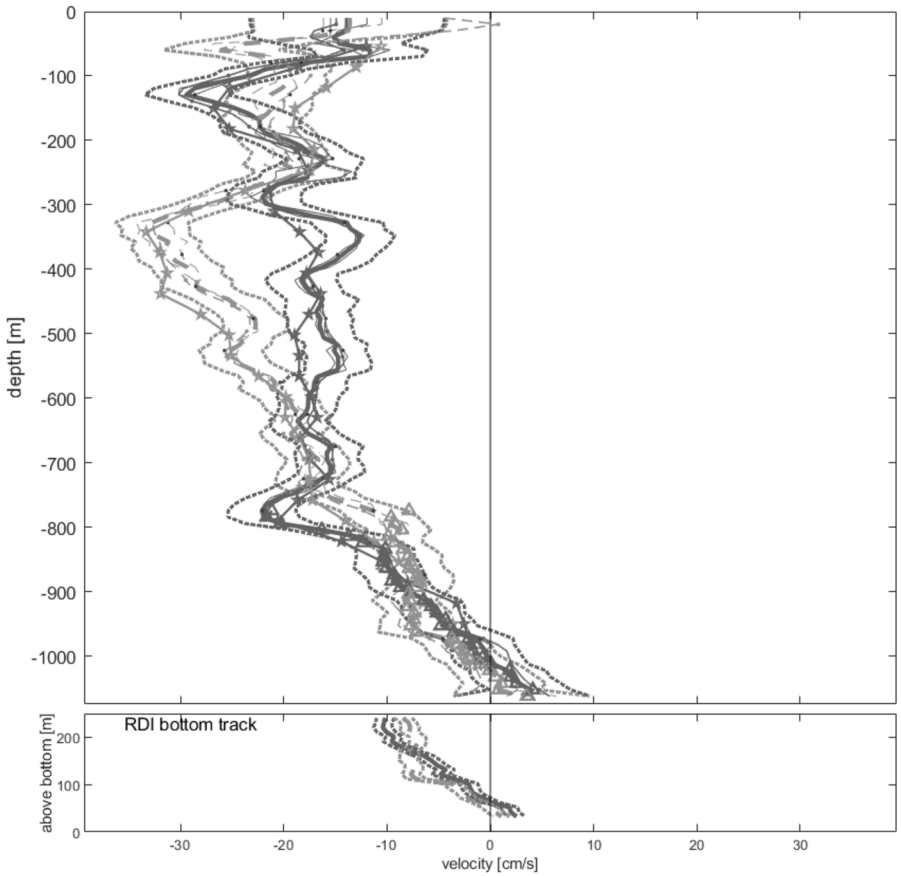

Fig. 5.7 Example of processed east-west (red) and north-south (green) velocities from lowered ADCP measurements at station 7. Dotted lines are error estimates. The stars are the velocities measured with the OS38 shipboard ADCP.

The instruments were used on the MSM83 cruise where no problems where problems with water intrusions were observed. On the MSM85 the same devices were used without any problems. LADCP measurements were only carried on stations deeper than 500 m. The data processing was carried out with the LDEO toolbox version IX.13 by the University of Columbia during the cruise using an inverse method, incorporating bottom track velocities, CTD measurements and OS38 Shipboard-ADCP measurements. The data collected at station 127 could not be used due to low battery voltage.

5.5 Biogeochemistry of Trace Gases

Daniel Bastian, Damian L. Arévalo-Martínez (not on board), H. W. Bange (not on board), Carolin. R. Löscher (not on board)

5.5.1 Background and Goals

Subpolar/polar ecosystems are particularly sensitive to climate change and therefore the projected increases in temperature and light penetration (including UV radiation) are likely to alter its ecosystem structure and function, which will in turn feedback on climate. Nitrous oxide (N_2O) and methane (CH_4) are potent greenhouse gases and as such it is timely to investigate their distribution, air-sea fluxes and production pathways in high-latitude ecosystems, in particular because of the poor temporal and spatial coverage of available measurements. The same applies for the indirect greenhouse gas carbon monoxide (CO), which is largely neglected in global budgets despite observations showing a strong source in marine surface waters.

Our major goals during the expedition were to: *i)* decipher the water column distribution of N_2O and CH_4, *ii)* infer their main formation mechanisms, and *iii)* investigate the air-sea dynamics of N_2O, CH_4 and CO. Likewise, in conjunction with other WP's we hope to be able to provide insights on the role of biology and ocean circulation on the production/consumption and overall budget of these gases on the east Greenland shelf, as well as the impact of sea ice melting on the emission of trace gases. To this end, we combined several approaches for along-track and discrete measurements of trace gases and carried out 3 incubation experiments at selected locations.

5.5.2 Continuous Surface Measurements

Underway measurements of dissolved N_2O and CO in seawater were carried out by means of an autonomous equilibrator headspace setup coupled to a trace gas analyzer based on off-axis integrated cavity output spectroscopy (OA-ICOS; Los Gatos Research Inc., USA). The combined setup is shown in Fig. 5.8. Seawater was drawn from about 6 m depth into the system by using a submersible pump installed at the ship's hydrographic well. Control measurements and calibration procedures were performed every 8 h by means of 3 standard gas mixtures (Deuste Steininger GmbH, Germany) bracketing the expected concentrations in this area. Atmospheric measurements of N_2O and CO were conducted every 8h by drawing air from the ship's mast.

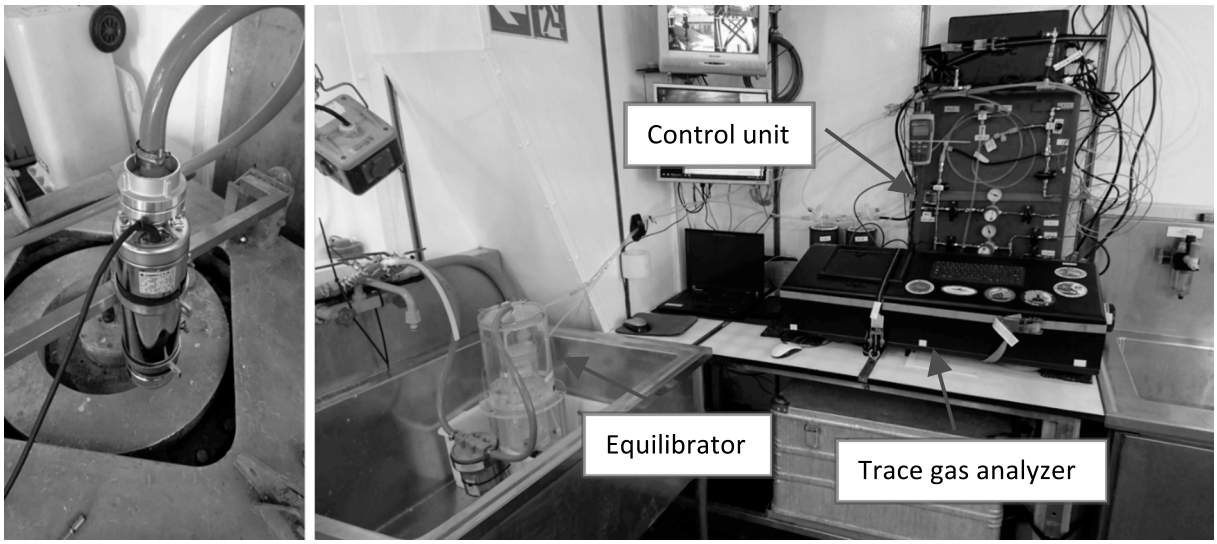

Fig. 5.8 System for continuous monitoring of trace gases during MSM85. The left panel shows the submersible pump installed at the ship's hydrographic well. The right panel shows the equilibration chamber, in which continuously flowing surface waters were equilibrated with a fixed amount of air in order to measure the amount of dissolved gas along the cruise track. Moreover, the spectroscopic analyzer for N_2O and CO measurements and its control unit are shown (photo credit: Damian L. Arévalo-Martínez).

5.5.3 Discrete Sampling

a) Underway surface sampling

In addition to the continuous N_2O and CO measurements, regular discrete CH_4 surface water samples have been obtained to investigate the sea-air-fluxes of this gas in the study area. Overall about 100 vials have been filled for this.

b) Water column sampling

In order to decipher depth distribution and cycling of N_2O and CH_4 in this area, seawater samples were collected during several CTD stations. Overall 23 stations on 8 transects have been sampled in 8 to 10 depths (approximately 1300 samples) to resolve the most important cross-shore gradients and the main features of the water column distribution. For both gases, bubble-free triplicate samples were collected and immediately sealed by means of butyl stoppers and aluminum crimps. Subsequently 50 µL of a saturated mercuric chloride ($HgCl_2$) solution were added. The samples will be analyzed by means of a headspace equilibrium method and gas chromatographic analysis at the chemical oceanography department of GEOMAR. In order to determine the presence and abundance of functional gene markers of nitrogen and carbon cycling, samples were collected at selected locations and the same depths at which inorganic nutrients and trace gases samples were collected. Sample processing consisted in filtering water from selected depths into Durapore® membrane filters (0.22 µm) which were immediately frozen at -80°C. In all stations with molecular work, samples for flow cytometry analysis were also taken. The molecular analysis will be carried out by Carolin Löscher at the biology department of the University of Southern Denmark. An overview of the sampling locations is shown in Fig. 5.9.

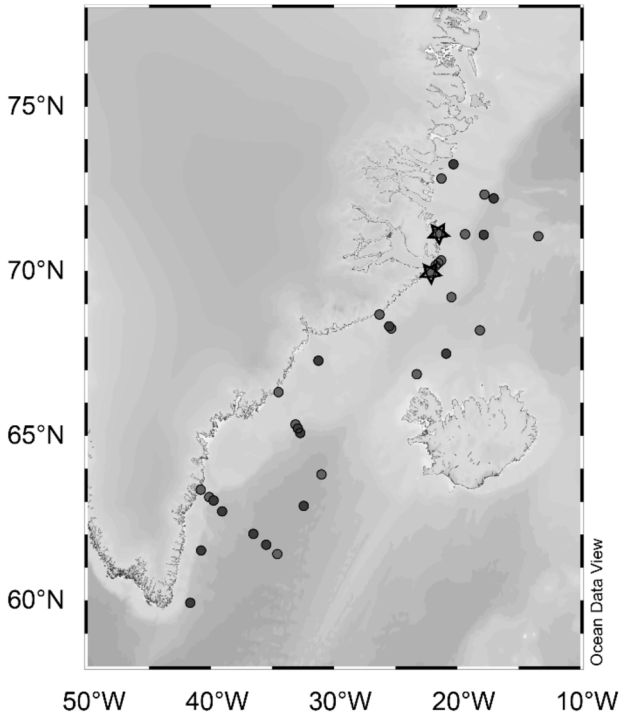

Fig. 5.9 Sampling and experiment locations for trace gases during MSM85. The red dots indicate stations where samples for depth profiles of N_2O, CH_4 and functional gene markers were collected, whereas the blue dots indicate the CH_4 sampling for surface waters. Stars show the sampling locations in which incubation experiments were conducted.

5.5.4 Incubation Experiments

In order to quantify carbon uptake in the study area two ^{13}C incubation experiments were carried out during the cruise. For this, surface water samples were taken from the CTD/rosette from which one background sample of 2 L was filtrated directly on to pre-combusted GF/F filters and dried in a 50 °C oven for 12 h and then stored in vials. The incubation was conducted via addition of 1 mL of pre-dissolved ^{13}C-HCO_3^- in 1 L sample water as triplicates, respectively. The triplicates were then incubated for 24 h in the incubation device of the Trace Metals Group under natural light conditions. Temperature data was continuously recorded by the ship's thermosalinograph. After incubation the triplicates were filtered onto pre-combusted GF/F filters, which were then dried at a 50 °C oven for at least 12 h and subsequently were stored. The molecular analysis will be carried out by Carolin Löscher at the biology department of the University of Southern Denmark.

5.5.5 Expected Results

The field work conducted during the MSM85 cruise will provide:

i) The first data-based regional estimate of the air-sea fluxes of N_2O, CO and CH_4 and its overall importance for the subpolar North Atlantic.
ii) A comprehensive view of the large-scale water column distribution of N_2O and CH_4, for the region. Together with the hydrographic and chemical information collected by other groups this will help elucidating trace gas transport pathways towards and from the Arctic and its main production/consumption processes.
iii) Novel data on the dynamical balance between biology and circulation for the production/consumption of trace gases in the subpolar North Atlantic.

5.6 Microbial Responses to the Release of Dissolved Organic Carbon

Alba Filella, Mark Hopwood (not on board), Anja Engel (not on board)

5.6.1 Background and Goals

Ice and water discharge from the Greenland ice sheet (GrIS) has more than double from 1983 to 2003 as a response of both oceanic and atmospheric forcing. The associated freshening of coastal waters has induced physical and biogeochemical changes that potentially affect productivity, element cycling, vertical supply of nutrients and carbonate chemistry. Nonetheless the individuality, complexity and inaccessibility of glacial systems have limited the number of studies exploring these coastal Arctic marine ecosystems.

The east Greenland current (EGC) exits the Arctic circumpolar current and meanders around the East Greenland shelf transporting high levels of organic matter (OM) south from Fram Strait. Arctic organic matter is mainly derived from riverine runoff (soil-derived, highly degraded, nitrogen-poor complex carbon substances) occurring along the Siberian shelf and discharging into the Arctic Circumpolar Current where it accumulates.

Dissolved organic matter is the largest active reservoir of reduced carbon in the ocean estimated to be equivalent in size to the atmospheric CO_2 pool. With increased warming and water stratification across the Arctic on decadal timescales, primary productivity could be shifting towards a dependence on allochthonous inputs and local mineralization. Therefore, biological and abiotic processes that could transform DOC properties or alter the fluxes of terrestrial DOC into Arctic Waters should be further investigated in order to understand the cycling and fate of OC in those areas.

10% of the global DOC pool is contained in hydrogels, a dynamic continuum of organic polymer particles formed by the aggregation and coagulation of extracellular organic polymers released mainly by phytoplankton and bacteria. This process is of great importance for carbon cycling since it links the DOC pool (colloids) with the particulate OC pool and affects the magnitude of the POC sink. Yet there is limited data on hydrogel distribution and behaviour in the Arctic. Community structure and bacterial activity primarily control production and turnover of the DOC and POC pools but in turn, the concentration and composition of DOC appears to feedback into the biological responses. The distribution of hydrogels across this dynamic region will therefore be investigated to gain insight into the relationships between community composition, environmental change and POC fluxes.

We hypothesize the studied system is influenced by several dissolved organic carbon (DOC) sources and thus our major aim is to quantify and characterize this dissolved carbon pool along the East Greenland shelf. Secondly, we will examine the associated communities (bacteria and phytoplankton) responses to distinct DOC and determine what consequences could arise regarding gel particle formation and further consumption or export of OC. Along the study region, local freshwater inputs from sea-ice melt and ice melt are coupled to complex physical dynamics that can influence nutrient distributions, light availability and thus seasonal productivity. Hence, we anticipate varying OC in some coastal regions such as enhanced decomposition of more complex humic-like-OC in regions of high primary production.

Overall, we would like to contribute to the global understanding of the Cryosphere to Ocean connection regarding processes and paths affecting OC carbon release by freshwater and the consequences will have on the microbial communities.

Table 5.2. CTD sampling summary. Stations ID, parameters and sampling depth are provided for each CTD samples. (ns: not sampled)

St.	DOC	CDOM/FDOM	Flow Cytometry	POC/PN	TEP	CSP	CLSM
msm85_002	162, 155, 131, 108, 69, 48, 39 and 25m	162, 155, 131, 108, 69, 48, 39 and 25m	162, 155, 131, 108, 69, 48, 39 and 25m	162, 155, 131, 108, 69, 48, 39 and 25m	162, 155, 131, 108, 69, 48, 39 and 25m	162, 155, 131, 108, 69, 48, 39 and 25m	162, 155, 131, 108, 69, 48, 39 and 25m
msm85_006	380, 194, 97, 38, 18 and 11m	380, 194, 97, 38, 18 and 11m	380, 194, 97, 38, 18 and 11m	380, 194, 97, 38, 18 and 11m	380, 194, 97, 38, 18 and 11m	380, 194, 97, 38, 18 and 11m	380, 194, 97 and 18m
msm85_013	2306, 1969, 1182, 964, 492, 242, 47, 27 and 12m	2306, 1969, 1182, 964, 492, 242, 47, 27 and 12m	2306, 1969, 1182, 964, 492, 242, 47, 27 and 12m	2306, 1969, 1182, 964, 492, 242, 47, 27 and 12m	2306, 1969, 1182, 964, 492, 242, 47, 27 and 12m	2306, 1969, 1182, 964, 492, 242, 47, 27 and 12m	2306, 964, 242, 47, 27 and 12m
msm85_016	2753, 1970, 986, 690, 95 and 32m	2753, 1970, 986, 690, 95 and 32m	2753, 1970, 986, 690, 95 and 32m	2753, 1970, 986, 690, 95 and 32m	2753, 1970, 986, 690, 95 and 32m	2753, 1970, 986, 690, 95 and 32m	2753, 1970, 986, 690, 95 and 32m
msm85_021	2679, 1970, 1184, 440, 196, 98, 47, 27 and 13m	2679, 1970, 1184, 440, 196, 98, 47, 27 and 13m	2679, 1970, 1184, 440, 196, 98, 47, 27 and 13m	2679, 1970, 1184, 440, 196, 98, 47, 27 and 13m	2679, 1970, 1184, 440, 196, 98, 47, 27 and 13m	2679, 1970, 1184, 440, 196, 98, 47, 27 and 13m	2679, 1970, 1184, 196, 98, 47, 27 and 13m
msm85_026	1478, 988, 792, 541, 98, 58, 27 and 5m	1478, 988, 792, 541, 98, 58, 27 and 5m	1478, 988, 792, 541, 98, 58, 27 and 5m	792, 541, 98, 58, 27 and 5 m	1478, 988, 792, 541, 98, 58, 27 and 5m	1478, 988, 792, 541, 98, 58, 27 and 5m	27 and 5m
msm85_039	245, 147, 97, 43, 24 and 10m	245, 147, 97, 43, 24 and 10m	245, 147, 97, 43, 24 and 10m	245, 147, 97, 43, 24 and 10m	245, 147, 97, 43, 24 and 10m	245, 147, 97, 43, 24 and 10m	245, 147, 97, 43, 24 and 10m
msm85_041	89, 59, 39, 19 and 9m	89, 59, 39, 19 and 9m	89, 59, 39, 19 and 9m	89, 59, 39, 19 and 9m	89, 59, 39, 19 and 9m	89, 59, 39, 19 and 9m	ns
msm85_048	334, 218, 109, 47, 18 and 12m	334, 218, 109, 47, 18 and 12m	334, 218, 109, 47, 18 and 12m	334, 218, 109, 47, 18 and 12m	334, 218, 109, 47, 18 and 12m	334, 218, 109, 47, 18 and 12m	218, 109, 47, 18 and 12m
msm85_063	221, 167, 98, 38, 18 and 9m	221, 167, 98, 38, 18 and 9m	221, 167, 98, 38, 18 and 9m	221, 167, 98, 38, 18 and 9m	221, 167, 98, 38, 18 and 9m	221, 167, 98, 38, 18 and 9m	221, 167, 98, 38, 18 and 9m
msm85_064	27 and 12m	27 and 12m	27 and 12m	ns	ns	ns	ns
msm85_070	146, 28 and 13m	146, 28 and 13m	146, 28 and 13m	ns	ns	ns	ns
msm85_075	26m	26m	ns	26m	ns	ns	26m
msm85_087	144, 113, 55, 18 and 9m	144, 113, 55, 18 and 9m	144, 113, 55, 18 and 9m	144, 113, 55, 18 and 9m	144, 113, 55, 18 and 9m	144, 113, 55, 18 and 9m	144, 113, 55, 18 and 9m
msm85_088	295, 146, 46 and 9m	295, 146, 46 and 9m	295, 146, 46 and 9m	146, 46 and 9m	ns	ns	ns
msm85_091	75, 49, 35, 19 and 12m	75, 49, 35, 19 and 12m	75, 49, 35, 19 and 12m	75, 49, 35, 19 and 12m	75, 49, 35, 19 and 12m	75, 49, 35, 19 and 12m	75, 49, 35, 19 and 12m
msm85_099	456, 344, 295, 196, 95, 70, 39, 19 and 10m	456, 344, 295, 196, 95, 70, 39, 19 and 10m	456, 344, 295, 196, 95, 70, 39, 19 and 10m	196, 95, 39, 19 and 10m	196, 95, 39, 19 and 10m	196, 95, 39, 19 and 10m	196, 95, 39, 19 and 10m
msm85_114	811, 541, 315, 98, 39, 19 and 12m	811, 541, 315, 98, 39, 19 and 12m	811, 541, 315, 98, 39, 19 and 12m	541, 315, 98, 39, 19 and 12m	811, 541, 315, 98, 39, 19 and 12m	811, 541, 315, 98, 39, 19 and 12m	811, 98, 39, 19 and 12m
msm85_120	984, 459, 290, 97, 39 and 13m	984, 459, 290, 97, 39 and 13m	984, 459, 290, 97, 39 and 13m	97, 39 and 13m	984, 459, 290, 97, 39 and 13m	984, 459, 290, 97, 39 and 13m	ns
msm85_128	560, 314, 98, 48, 30 and 12m	560, 314, 98, 48, 30 and 12m	560, 314, 98, 48, 30 and 12m	560, 314, 98, 48, 30 and 12m	560, 314, 98, 48, 30 and 12m	560, 314, 98, 48, 30 and 12m	314, 98, 48, 30 and 12m
msm85_140	273, 197, 98, 48, 29 and 9m	273, 197, 98, 48, 29 and 9m	273, 197, 98, 48, 29 and 9m	273, 197, 98, 48, 29 and 9m	273, 197, 98, 48, 29 and 9m	273, 197, 98, 48, 29 and 9m	98, 48, 29 and 9m
msm85_149	163, 97, 49 and 12m	163, 97, 49 and 12m	163, 97, 49 and 12m	163, 97, 49 and 12m	163, 97, 49 and 12m	163, 97, 49 and 12m	163, 49 and 12m
msm85_154	255, 156, 97, 53, 35 and 12m	255, 156, 97, 53, 35 and 12m	255, 156, 97, 53, 35 and 12m	255, 156, 97, 53, 35 and 12m	255, 156, 97, 53, 35 and 12m	255, 156, 97, 53, 35 and 12m	255, 156, 97, 53, 35 and 12m
msm85_162	2458, 986, 494, 295, 96, 59 and 9m	2458, 986, 494, 295, 96, 59 and 9m	2458, 986, 494, 295, 96, 59 and 9m	986, 494, 295, 96, 59 and 9m	986, 494, 295, 96, 59 and 9m	986, 494, 295, 96, 59 and 9m	986, 494, 295, 96, 59 and 9m
msm85_166	492, 244, 99, 39, 19 and 8m	492, 244, 99, 39, 19 and 8m	492, 244, 99, 39, 19 and 8m	492, 244, 99, 39, 19 and 8m	99, 39, 19 and 8m	ns	492, 99, 39, 19 and 8m
msm85_168	1424, 99, 34 and 13m	1424, 99 34 and 13m	1424, 99, 34 and 13m	ns	ns	ns	ns

5.6.2 Work Program

The MSM85 sampling plan was designed in a way that would capture a great area of the East Greenland System, passing through highly variable environments and physical regimes within the system. Thus in order to investigate and answer the main questions addressed in this section, at every planned transect the coastal and eastern most stations were sampled to resolve the most important cross-shore gradients. Intermediate stations were then selected at regular intervals to produce cross-shelf gradients. Discrete sampling of distinct depth profiles was done for each marked station (26 red points) on the map (Fig. 5.10).

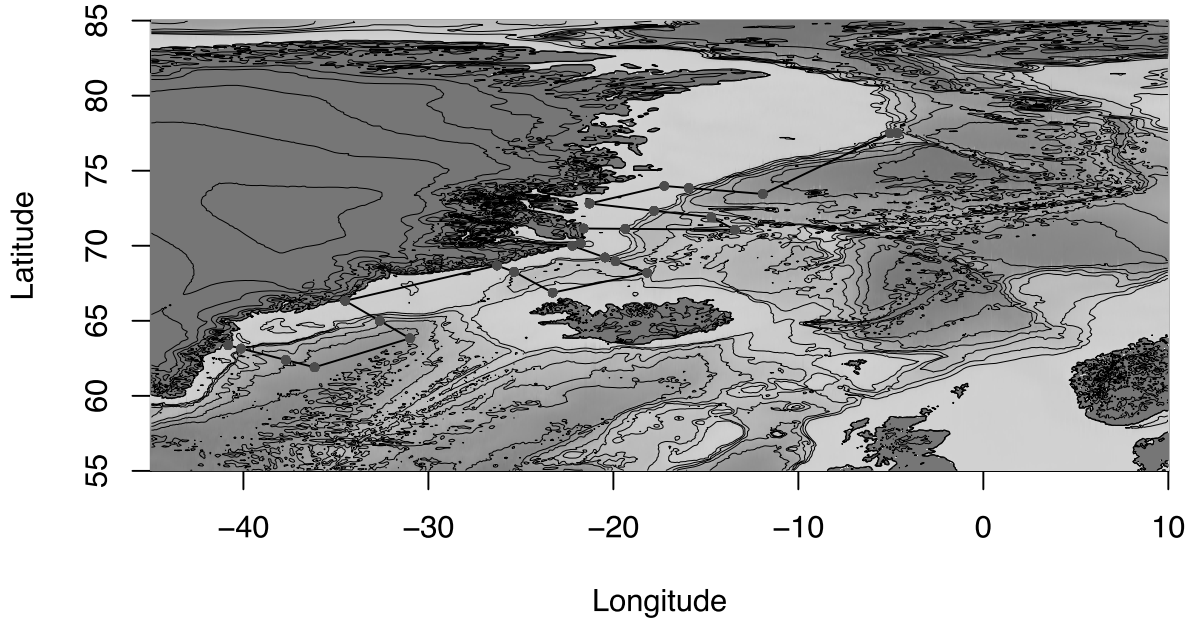

Fig. 5.10 Sampling locations for organic carbon and biological parameters during MSM85. Generally for each sampled station (red dots) depth profiles were collected for DOC, CDOM, FDOM, POC/PN, Flow Cytometry, TEP, CSP and CLSM.

Generally, depth and sampling resolution at each station were decided depending on the bottom depth and main features of the water column. For shelf and shallow areas around 5-6 depths were taken, increasing to 7-9 depths for deeper zones (Table 5.2).

Seawater was collected in 4L plastic bottles from the Niskin bottles mounted on the rosette (Fig. 5.12, left) and used immediately after sampling (if not, stored in between in the fridge) for collecting DOC, CDOM, FDOM, POC/PN, Flow Cytometry, TEP, CSP and CLSM samples in the wet lab (Fig. 5.11).

Samples processing was performed in a specific order depending on the sensitivity and possibility of contamination of the measured parameters. Starting with DOC (CDOM/FDOM), 20mL (40mL) were collected into pre-combusted glass ampoules (amber-glass vials) after filtering through 0.45µm GMF (CHROMAFIL XTRA PES-45/25) syringe filters. DOC ampoules were then acidified with 20µL of 30% hydrochloric acid, flame sealed and all DOC and CDOM/FDOM vials were then stored in the dark at 4-5ºC.

Fig. 5.11 General overview of the wet lab during MSM85, showing on the first plain the filtration track used for collecting POC/PN and chlorophyll a samples. The right panel is a close up of the area where TEP, CSP and CLSM were filtered and stained. Measurements for CDOM, FDOM, DOC and Flow Cytometry were also performed between the area on the right panel and under the fume hood.

Fig. 5.12 On the left panel sampling from the CTD for biological and biochemical parameters during MSM85 is shown. The right panel display sampling place and procedure for CDOM and FDOM.

On second place, triplicates of seawater (1.8mL) were added to a 2mL cryovials for bacteria, phytoplankton and viruses counts containing 85µL (34µL for viruses) of 25% glutardialdehyde (GDA). Afterwards the tubes were incubated for 15-30 min at 4ºC, immediately flash-frozen in liquid nitrogen and stored at -80ºC.

In between the first measurements, filtration of 1000-1500mL seawater for particulate organic carbon and nitrogen (POC/PN) onto combusted (8h at 500ºC) GF/F filters (Whatmann, 25 mm) was performed in duplicates. After transport to GEOMAR, the filters will be exposed to hydrochloric acid overnight, dried at 60ºC for 12h and then will be analysed for C and N content using CHN analyser (euro EA, Hechatech) following the procedure described by Sharp (1974).

The concentration and distribution of gel particles (TEP and CSP) will be examined colorimetrically after Passow and Alldredge (1995). For each sampled station and depth a set volume of 100mL was filtered in triplicate using low and constant vacuum (<200mbar) onto 0.4µm Nucleopore filters (25 mm) for each kind of particle. The filters are then stained with 1mL Alcian Blue for TEP and 1mL Comassie Brilliant Blue for CSP for 5 seconds. Finally both sets of filters were rinsed with 15 mL of Milli-Q water to remove any excess dye and then stored frozen at -20ºC until analysis.

The remaining volume was used to analyse aggregate composition and bacteria abundances associated with particles by the method Confocal Laser Scanning Microscopy (CLSM). For that, 30 mL duplicates were filtered onto 0.2µm black polycarbonate filters (25 mm) and stored at -20ºC.

5.6.3 Expected Results

DOC cycling is still regarded as a complicated topic to assess due to the heterogeneous mixture of organic compounds that are in turn affected by many processes simultaneously. The collection, processing and interpretation of the samples acquired during the campaign MSM85 will contribute to comprehend processes leading to the observed OC composition and distribution.

i) Organic carbon in the East Greenland System

Different signatures of OC will be distinguished along the studied area. High amounts of refractory DOC with traces of iron coming from the Arctic Basin are carried by the EGC, although the southern limit of this is unclear. In the southernmost coastal area sources of OC could differ depending on the type of glacier dominating runoff in the region: melting of land-terminating glaciers (surface runoff) will carry low DOC and a great fraction might be non labile. On the other hand, downstream of large marine-terminating glaciers (such as Sermilik), then enhanced upwelling of ambient deep water carrying high amounts of nutrients and deep DOC is expected and may influence coastal OC and nutrient distributions. Accompanying the later process, enhancement of productivity by nutrients could also lead to the production of amino acid like OC (labile OC) in the area.

ii) Microbial communities and their responses to different OC sources

Flow cytometry measurements for each station and depth will provide bacterial, phytoplankton and viruses abundances. In that way, a rough estimation on how microorganisms are distributed and contribute to the whole community within different water masses will be achieved.

Lability of OC together with inorganic nutrients availability might be the main driver affecting bacterial activity and thus their abundances. Consequently wherever the system is influenced by humic-like OC or low OC content, bacteria activity might be limited (e.g. Polar surface waters or downstream of areas receiving high volumes of runoff from land-terminating glaciers). Phytoplankton blooms will (similarly to bacteria) occur in productive areas and competition for inorganic nutrients between autotrophs and heterotrophs is also expected.

Furthermore, top down control on bacteria by viruses is predicted to be relevant during summer (specially after bloom conditions), which will be checked when calculating virus to bacteria ratios.

iii) TEP and CSP distributions

Gel particles are still not incorporated in all regular field samplings and few data is available. Previous studies are restricted to Fram Strait and generally the patters appear to be similar: higher concentrations of TEP are found in within the Atlantic Water (easternmost stations (offshore) in our case). However, coastal distributions of gel particles around Greenland are less known: we speculate that their concentrations will vary greatly depending on the productivity of the fjord systems possible showing local differences. Microbial bloom dynamics are also very coupled with the magnitude and distribution of TEP and CSP along the water column. It has been shown that TEP production increases towards the end of the bloom but conversely CSP appear to reach higher concentrations during the exponential growth of phytoplankton, when cells have still enough nutrients to growth. Therefore CSP is foreseen to correlate with chlorophyll a and TEP with particulate OC.

Concluding, we predict a disparity between TEP and CSP concentrations and distribution along the water column, which will be highly influenced by the phytoplankton bloom phase and microbial group abundances.

5.7 Nutrients, Trace Metals and Phytoplankton Communities

(Insa Rapp, Alba Filella, Karl Purcell)

5.7.1 Background

Besides major macronutrients (N, P, and Si), trace elements such as iron (Fe), cobalt (Co) and manganese (Mn) are essential micronutrients for phytoplankton and their availability controls marine carbon and nitrogen cycling in large parts of the ocean including the High Latitude North Atlantic (Moore et al., 2013). Offshore of the southern East Greenland Coast, phytoplankton growth has been shown to be limited by the micronutrient iron (Nielsdottir et al., 2009; Ryan-Keogh et al., 2013), whereas further north along the East Greenland Coast, phytoplankton growth was observed to be limited by nitrogen (unpublished data). Alongside these nutrients, co-limitation of phytoplankton growth by vitamin B_{12} has recently been reported in the Arctic and Antarctic (Browning et al., 2017; Bertrand et al., 2007, 2012). An increase in discharge from the Greenland Ice Sheet likely impacts the nutrient inventory and nutrient stoichiometry around Greenland and may consequently have a strong impact on primary production and phytoplankton community composition in this region (Hawkings et al., 2015). However, exactly how glacial meltwater input will change primary production, and the types of phytoplankton communities undertaking this primary production, is uncertain (Arrigo et al., 2017, Hopwood et al., 2018). The objectives of our work on the MSM85 cruise were, therefore, to assess the influence of discharge from the Greenland Ice Sheet on macro- and micronutrient distributions, to investigate the potential for nitrogen fixation in this region and to investigate the phytoplankton community response to gradients in these nutrients.

5.7.2 Methods

Trace Metal Clean Surface Seawater Acquisition. Underway surface water samples were collected with a trace metal clean surface water sampling device (tow fish), which was deployed at 2-3 m at 66 locations along the cruise transect for multiple parameters (Fig. 5.13, Table 7.2). The seawater was pumped through acid-cleaned PVC tubing using a Teflon bellows pump into a

trace metal clean area in the lab. The trace metal clean area was created by a clean bench which filters air through a Hepa filter into an area which is separated from the rest of the lab with plastic sheets, creating an overpressure.

Nutrient sampling. Surface samples for major nutrients were filtered by an 0.8/0.2 µm Acropak 1000 cartridge filter and collected in 15 mL Falcon tubes (after 3 rinses). Nutrient samples from depths profiles were collected in regular intervals (Table 7.3). The samples were collected from the Niskin bottles into a 60 mL syringe (rinsed 3 x with ~20 mL of seawater) and filtered using a PES syringe filter (0.2 µm) and collected into a 15 mL Falcon tubes after discarding the first 20 mL of filtrate and rinsing the sample tube three times with filtrate. The samples were acidified in the same way as surface samples. Surface and station samples were acidified by adding 20 µL of concentrated HCl (Optima grade, Fisher) within 24 hours of sampling. Samples were stored refrigerated between sampling and acidification and at room temperature after acidification and shipped to Geomar, Kiel for later analysis for nitrate, phosphate and silicic acid in the lab.

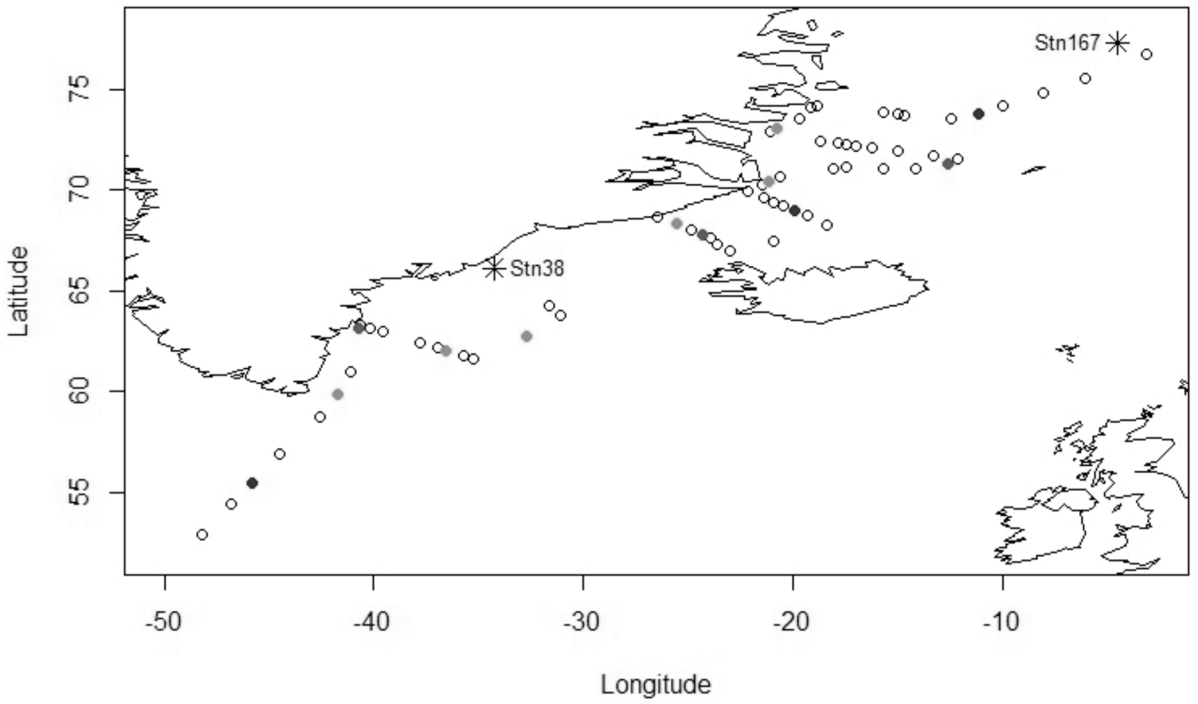

Fig. 5.13 Map of surface samples collected using towed fish and experiments. Black open circles: underway sampling for trace metals and nutrients. Green filled circles: additional sampling for RNA, DNA, proteins, vitamin B_{12}, flow cytometry, chlorophyll *a* (chl *a*), dissolved organic carbon (DOC), particulate organic carbon (POC), coloured and fluorescent dissolved organic matter (cDOM and fDOM), transparent exoplymer particles (TEP) and coomassie stainable particles (CSP); blue filled circles: additional sampling/setting-up of experiments for N_2 fixation rates and primary production; red filled circles: additionally nutrient incubation experiments set up with additions of nitrogen (NO_3 + NH_4), iron and B_{12}. Stars show location of stations where samples were collected at four depth for chl a, FCM, RNA, DNA and proteins and B_{12}.

Trace metal sampling. Dissolved trace metal samples were collected from the tow fish filtered using an 0.8/0.2 µm Acropak 1000 cartridge filter and collected into acid-cleaned 125 mL LDPE bottles). Total dissolvable samples were collected unfiltered. All trace metal samples were

acidified to ~pH 1.9 by adding 150 µL of concentrated HCl (Optima grade, Fisher). The samples will be processed at Geomar by pre-concentration using a SeaFAST device and analyzed simultaneously for Fe, Co, Mn, Cd, Ni, Zn, Cu and Pb by ICP-MS (Rapp et al., 2017).

Vitamin B_{12} sampling. Vitamin B_{12} samples were collected unfiltered from the tow fish into 2 x 1L opaque HDPE bottles, NH_4formate (Optima grade) was added to a concentration of 0.5 mM and biotin and riboflavin to a concentration of around 50 ng/L. The sample was transferred into a 2L Flexboy and filtered by gravity in a cold room (5°C) at dark using a Sterivex filter to extract the particulate B_{12} fraction, followed in-line by an Agilent Bond Elut cartridge (pre-cleaned with Ethanol and 0.1 M HCL) to retain the dissolved B_{12} fraction. The filters were stored at -80°C and the cartridges at -20°C until analysis at Geomar. At two locations samples for vitamin B_{12} were collected at four depths from the CTD stations (Fig. 5.13, Table 7.3). The samples were directly collected from the Niskin bottes into 2 L Flexboys and NH_4formate, Biotin and Riboflavin were added at the same concentrations as for surface samples and were processed in the same way.

Chlorophyll a sampling. 100-150 mL samples were filtered onto GFF filters (MF300, Fisher) and stored at -80°C until analysis at Geomar.

Flow cytometry sampling. 1.725mL of seawater were added to 2 mL Cryovials containing 0.115mL 16% paraformaldehyde yielding a final paraformaldehyde concentration of 1%. Samples were mixed by inverting a few times and incubated for 10 minutes at room temperature in the dark before being transferred to -80°C. Samples will be analysed for nanophytoplankton, picophytoplankton, Synechococcus, Prochlorococcus and total bacterial cell counts on a FACSort flow cytometer (Beckton-Dickinson, UK) following the method of e.g. Davey et al. (2008).

RNA, DNA and protein sampling. Unfiltered seawater was collected from the tow fish or Niskin bottles into 20 L or 10 L Carboys and filtered for RNA, DNA and protein samples in a cold room at 5 °C. Samples were filtered at a flow rate of 50–100 mL/min onto 3µm and 0.2 µm 45 mm polycarbonate (PC) filters connected inline. Samples for RNA were filtered as soon as possible after sampling using approximately 1 L of seawater per sample. For protein samples, 3-9L of seawater were filtered after collection of RNA samples and DNA samples were filtered last using around 2 L of seawater per sample. All filters were placed into 2 mL Cryovials immediately after filtration, submerged into liquid nitrogen and stored at -80°C until analysis at Dalhousie University. Filter lines are rinsed with 1M HCl and Milli-Q before filtration of the next sample.

Nutrient incubation experiments. Three incubation experiments were carried out using seawater collected trace metal-clean from the tow fish described above. For each experiment 24 acid-cleaned 1L polycarbonate (PC) bottles were filled over approximately 30 minutes during transit. Apart from three control bottles, bottled seawater was spiked with the following combinations of nutrients/trace metals in triplicates: Nitrogen (N), Fe, vitamin B_{12}, N+Fe, N+vitamin B_{12}, Fe+vitamin B_{12}, N+Fe+vitamin B_{12}. Final concentrations of added nutrients were 2µM NO_3+1µM NH_4 for N additions, 2 nM for Fe and 100 pM for vitamin B_{12}. Initial conditions were sampled in 1L bottles for all experiments at the beginning, middle and end of the bottle filling procedure and sampled for chlorophyll *a* and flow cytometry as described above. Bottles were sealed with parafilm and placed in ziplock bags in an incubator on-deck connected to the ships underway flow-through system to continuously maintain temperatures at that of sea surface waters. The lid and sides of the incubator were covered with Blue Lagoon screening (Lee

Filters), which maintained irradiance at ~30% of that of the surface. Bottles were removed from the incubator after ~72 hours and samples were collected from each bottle for chlorophyll *a* and flow cytometry. The remaining volume of each bottle was then filtered for DNA/proteins as described above.

Nitrogen fixation experiments. Alongside incubation experiments and at three additional locations (Fig. 5.13), experiments to determine nitrogen fixation rates were performed. For each experiment five acid-cleaned 4L PC bottles and one 1L PC bottle were filled with unfiltered seawater from the tow fish and an additional acid-cleaned PC bottles was filled with at least 2 L of filtered (0.8/0.2 µm Acropak 1000 cartridge) seawater. The bottles were stored at 5°C until further processing. The filtered seawater was degassed using two Mini Module membrane contactors connected in-line, attached to a peristaltic pump for the seawater flow and a vacuum pump attached to the gas outlets. The degassed seawater was directly collected in a 1L Tedlar bag and spiked with about 20 mL of $^{15}N_2$ gas. The gas bubble was dispersed into very small bubbles over a period of about one hour for dissolution and equilibration of the labelled nitrogen gas. Afterwards, three of the filled 4 L bottles were spiked with 1.7 mL of a ^{15}C-bicarbonate (1g/50 mL) solution and 250 mL of the $^{15}N_2$- enriched seawater. The bottles were then filled to the rim using seawater from the additional 1L bottle and closed with Septum Caps excluding any air bubble. A fourth bottle without any addition was filled the same way and served as a Control. Enriched and Control bottles were then placed into the incubator for 24 hours. An aliquot of 2-4L of the fifth bottle without any addition was filtered directly onto a pre-combusted 25 mm Advantec MF-75 glas fiber filter. The filter was dried at 60°C overnight and transferred to a pre-combusted glass-vial and stored at room temperature in the dark until analysis at Dalhousie University.

After taking out the bottles from the incubator, the three enriched bottles were slightly overpressurised using Helium gas (Ultra High Purity Grade - HE 5.0, Praxair) and two liquid samples per bottle were collected using a two-way needle into 12 mL exetainers which were previously spiked with 100 µL of saturated mercuric chloride solution and flushed with Helium gas. Afterwards 2-4 L of the each bottle (enriched and Control) were filtered onto pre-combusted Advantec filters and dried as described above.

5.8 Multibeam Echosounder

(Katharina Unger Moreno)

The aim of the multibeam echosounder on board are high resolution bathymetry maps. The data acquisition started on July 24th and ended on August 12th 2019. The depth varied between 70 m and 3000 m. For the aquisition of bathymetric data a hull mounted multibeam system from Kongsberg was used, the Kongsberg Simrad system EM122. There are two multibeam systems from Kongsberg installed on MARIA S. MERIAN, EM 122 and EM 710. During this cruise the EM 122 was mostly used, because it has a good resolution for depths between 10 m and 1000 m. The EM 710 is able to work until a depth of 2000 m but it can interfere with the underway ADCP measurement.

The multibeam echosounder uses a swath of beams giving off-track depth. The water depth is measured by the two way travel time of individual beams. There are two components, a transmitter and a receiver which are installed below the vessel. These arrays are perpendicular to each other (Mills Cross). The EM122 has a frequency of 12 kHz and a swath width up to 150°,

theoretically it can cover 6 time the water depth but during this cruise around 4 times the water depth was covered. The opening angle determines the lateral resolution, which gets less with shallow water depth. High density mode creates 432 soundings out of 288 beams. The emission beam is 150° across track and 1° along track. The receiver is 2° across track and 20° along track. A single beam has a dimension of 1° by 2°.

The system has to be calibrated through sound velocity profiles because of refraction of the non-vertical beams. The sound velocity profiles were updated whenever there was a major change in the physical properties of the water column, for example when MARIA S. MERIAN was near places having a lot of fresh water income. The sound velocity profiles where acquired through CTD downcast measurements. The software program MB-Systems (MultiBeam) was employed to processes the obtained data and when necessary to edit/clean it. GMT (Generetic mapping tool) was used for gridding and visualization.

6 Ship's Meteorological Station

(C. Mertens)

Meteorological data were collected automatically by the meteorological station of MARIA S. MERIAN, that is operated by the DWD (Deutscher Wetterdienst). High wind speeds, exceeding 20 m/s occurred on July 30 to 31, while the ship was working along the second CTD section in the Irminger Sea.

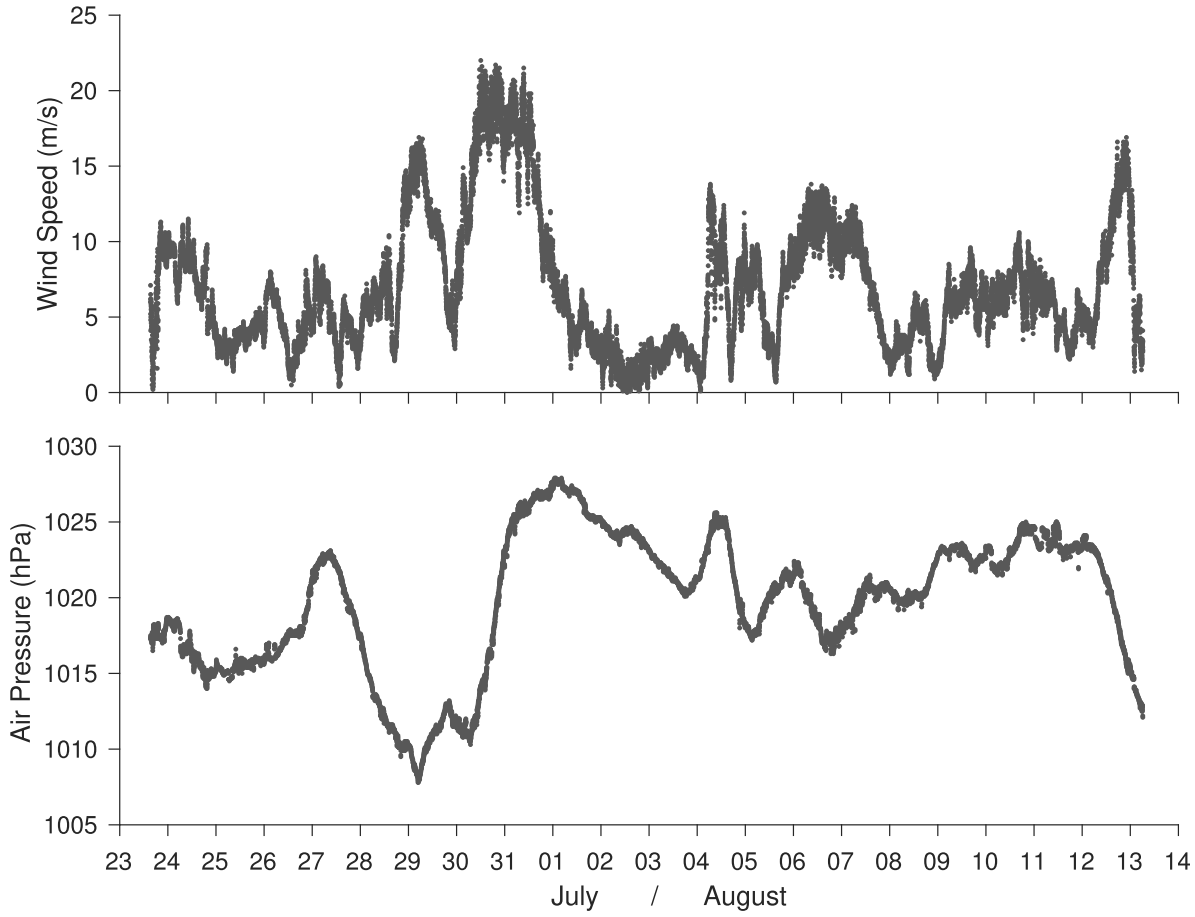

Fig. 6.1 Wind speed and air pressure during cruise MSM85 from the ship's meteorological station.

7 Station List MSM85

7.1 Overall Station List

Station No.	Gear	Time (UTC)	Latitude	Longitude	Depth (m)	Remarks
MSM85_1-1	Towfish	2019-07-23 19:18	47° 37,914' N	052° 34,558' W	178.3	in the water
MSM85_2-1	CTD/ROS	2019-07-27 08:32	63° 21,996' N	040° 49,020' W	175.1	
MSM85_3-1	CTD/ROS	2019-07-27 10:06	63° 18,747' N	040° 38,669' W	200.1	
MSM85_4-1	CTD/ROS	2019-07-27 11:14	63° 15,464' N	040° 28,381' W	307.4	
MSM85_5-1	CTD/ROS	2019-07-27 12:26	63° 12,245' N	040° 17,926' W	426.2	
MSM85_6-1	CTD/ROS	2019-07-27 13:36	63° 08,976' N	040° 07,558' W	391.9	
MSM85_7-1	CTD/ROS	2019-07-27 15:00	63° 07,590' N	040° 03,010' W	1095.8	
MSM85_8-1	CTD/ROS	2019-07-27 16:29	63° 05,740' N	039° 57,205' W	1286.4	
MSM85_9-1	CTD/ROS	2019-07-27 18:31	63° 02,484' N	039° 46,864' W	1572.0	
MSM85_10-1	CTD/ROS	2019-07-27 21:13	62° 52,741' N	039° 15,797' W	1735.0	
MSM85_11-1	CTD/ROS	2019-07-28 00:04	62° 42,995' N	038° 44,667' W	2110.7	
MSM85_12-1	CTD/ROS	2019-07-28 03:15	62° 33,251' N	038° 13,578' W	2326.4	
MSM85_13-1	CTD/ROS	2019-07-28 06:30	62° 23,481' N	037° 42,527' W	2360.4	
MSM85_14-1	CTD/ROS	2019-07-28 09:42	62° 13,731' N	037° 11,416' W	2455	
MSM85_15-1	CTD/ROS	2019-07-28 12:57	62° 03,961' N	036° 40,357' W	2626.1	
MSM85_16-1	CTD/ROS	2019-07-28 16:19	61° 54,232' N	036° 09,244' W	2762.7	
MSM85_17-1	CTD/ROS	2019-07-28 19:41	61° 44,497' N	035° 38,198' W	2872.1	
MSM85_18-1	CTD/ROS	2019-07-28 23:18	61° 34,771' N	035° 07,176' W	2928.0	
MSM85_19-1	CTD/ROS	2019-07-29 03:03	61° 24,986' N	034° 35,950' W	2951.7	
MSM85_1-1	Towfish	2019-07-29 05:16	61° 25,549' N	034° 33,229' W	2949.7	on deck
MSM85_20-1	Towfish	2019-07-29 13:05	62° 33,405' N	032° 54,826' W	2903.6	in the water
MSM85_21-1	CTD/ROS	2019-07-29 21:44	63° 49,973' N	031° 00,006' W	2690.3	
MSM85_22-1	CTD/ROS	2019-07-30 01:09	64° 04,976' N	031° 21,087' W	2683.4	
MSM85_23-1	CTD/ROS	2019-07-30 04:34	64° 19,986' N	031° 42,041' W	2579.5	
MSM85_20-1	Towfish	2019-07-30 07:46	64° 32,452' N	031° 57,401' W	2429.6	on deck
MSM85_24-1	CTD/ROS	2019-07-30 08:15	64° 34,976' N	032° 03,053' W	2378.5	
MSM85_25-1	CTD/ROS	2019-07-30 12:37	64° 49,988' N	032° 24,055' W	2045.9	
MSM85_26-1	CTD/ROS	2019-07-30 15:44	64° 59,985' N	032° 38,086' W	1791.1	
MSM85_27-1	CTD/ROS	2019-07-30 17:46	65° 05,000' N	032° 45,090' W	1632.9	
MSM85_28-1	CTD/ROS	2019-07-30 19:56	65° 11,976' N	032° 54,866' W	1322.4	
MSM85_29-1	CTD/ROS	2019-07-30 21:40	65° 16,907' N	033° 01,932' W	1008.1	
MSM85_30-1	CTD/ROS	2019-07-30 23:08	65° 20,977' N	033° 07,420' W	625.1	
MSM85_31-1	CTD/ROS	2019-07-31 00:28	65° 25,473' N	033° 13,750' W	270.0	
MSM85_32-1	CTD/ROS	2019-07-31 01:40	65° 29,989' N	033° 20,003' W	256.0	
MSM85_33-1	CTD/ROS	2019-07-31 03:30	65° 39,991' N	033° 34,010' W	305.7	
MSM85_34-1	CTD/ROS	2019-07-31 05:19	65° 49,997' N	033° 48,096' W	328.1	
MSM85_35-1	CTD/ROS	2019-07-31 06:55	65° 59,991' N	034° 02,047' W	256.5	
MSM85_36-1	CTD/ROS	2019-07-31 07:54	66° 04,988' N	034° 09,071' W	269.1	
MSM85_37-1	CTD/ROS	2019-07-31 08:56	66° 09,980' N	034° 16,066' W	274.7	
MSM85_38-1	CTD/ROS	2019-07-31 10:05	66° 14,986' N	034° 23,102' W	254.4	
MSM85_39-1	CTD/ROS	2019-07-31 11:23	66° 20,002' N	034° 30,118' W	309.8	
MSM85_40-1	Towfish	2019-08-01 07:56	68° 34,268' N	026° 41,676' W	198.9	in the water
MSM85_41-1	CTD/ROS	2019-08-01 09:06	68° 40,988' N	026° 17,539' W	96.5	
MSM85_42-1	CTD/ROS	2019-08-01 10:03	68° 38,786' N	026° 12,672' W	164.5	
MSM85_43-1	CTD/ROS	2019-08-01 10:46	68° 36,734' N	026° 08,083' W	145.9	
MSM85_44-1	CTD/ROS	2019-08-01 11:40	68° 32,532' N	025° 58,892' W	293.3	
MSM85_45-1	CTD/ROS	2019-08-01 12:40	68° 28,324' N	025° 49,453' W	324.8	
MSM85_46-1	CTD/ROS	2019-08-01 13:41	68° 24,134' N	025° 40,199' W	296.5	
MSM85_47-1	CTD/ROS	2019-08-01 14:45	68° 19,981' N	025° 30,967' W	287.0	
MSM85_48-1	CTD/ROS	2019-08-01 15:48	68° 15,733' N	025° 21,674' W	343.9	
MSM85_49-1	CTD/ROS	2019-08-01 17:12	68° 11,527' N	025° 12,576' W	646.6	
MSM85_50-1	CTD/ROS	2019-08-01 18:21	68° 09,517' N	025° 08,081' W	882.6	
MSM85_51-1	CTD/ROS	2019-08-01 19:36	68° 07,340' N	025° 03,530' W	1049.8	
MSM85_52-1	CTD/ROS	2019-08-01 21:03	68° 03,228' N	024° 54,588' W	1250.3	
MSM85_53-1	CTD/ROS	2019-08-01 22:48	67° 56,900' N	024° 40,866' W	1415.9	

MSM85_54-1	CTD/ROS	2019-08-02 00:37	67° 50,557' N	024° 27,269' W	1463.0	
MSM85_55-1	CTD/ROS	2019-08-02 02:58	67° 44,385' N	024° 13,855' W	1331.3	
MSM85_56-1	CTD/ROS	2019-08-02 04:46	67° 38,033' N	024° 00,409' W	1080.2	
MSM85_57-1	CTD/ROS	2019-08-02 06:25	67° 31,746' N	023° 46,691' W	829.9	
MSM85_58-1	CTD/ROS	2019-08-02 07:55	67° 23,490' N	023° 40,380' W	583.1	
MSM85_59-1	CTD/ROS	2019-08-02 09:14	67° 16,235' N	023° 34,759' W	399.2	
MSM85_60-1	CTD/ROS	2019-08-02 10:16	67° 11,037' N	023° 30,596' W	262.6	
MSM85_61-1	CTD/ROS	2019-08-02 11:25	67° 04,339' N	023° 25,520' W	245.4	
MSM85_62-1	CTD/ROS	2019-08-02 12:37	66° 56,599' N	023° 19,733' W	239.2	
MSM85_63-1	CTD/ROS	2019-08-02 13:29	66° 52,504' N	023° 17,016' W	236.4	
MSM85_64-1	CTD/ROS	2019-08-03 01:30	68° 12,014' N	018° 09,954' W	571.8	
MSM85_65-1	CTD/ROS	2019-08-03 03:10	68° 21,201' N	018° 30,612' W	1478.7	
MSM85_66-1	CTD/ROS	2019-08-03 05:19	68° 30,382' N	018° 51,143' W	826.4	
MSM85_67-1	CTD/ROS	2019-08-03 07:07	68° 39,599' N	019° 11,719' W	1100.0	
MSM85_68-1	CTD/ROS	2019-08-03 09:18	68° 48,685' N	019° 32,308' W	1300.1	
MSM85_69-1	CTD/ROS	2019-08-03 10:52	68° 53,341' N	019° 42,606' W	1456.9	
MSM85_70-1	CTD/ROS	2019-08-03 12:32	68° 57,980' N	019° 52,934' W	1548.1	
MSM85_71-1	CTD/ROS	2019-08-03 14:13	69° 02,550' N	020° 03,236' W	1506.9	
MSM85_72-1	CTD/ROS	2019-08-03 15:50	69° 07,077' N	020° 13,510' W	1275.4	
MSM85_73-1	CTD/ROS	2019-08-03 17:20	69° 09,282' N	020° 18,639' W	1082.0	
MSM85_74-1	CTD/ROS	2019-08-03 18:39	69° 11,520' N	020° 23,758' W	810.0	
MSM85_75-1	CTD/ROS	2019-08-03 19:39	69° 13,155' N	020° 27,125' W	580.0	
MSM85_76-1	CTD/ROS	2019-08-03 20:44	69° 16,377' N	020° 34,045' W	373.3	
MSM85_77-1	CTD/ROS	2019-08-03 21:34	69° 18,608' N	020° 39,145' W	369.6	
MSM85_78-1	CTD/ROS	2019-08-03 22:24	69° 20,913' N	020° 44,339' W	370.0	
MSM85_79-1	CTD/ROS	2019-08-03 23:29	69° 25,473' N	020° 54,635' W	404.7	
MSM85_80-1	CTD/ROS	2019-08-04 00:35	69° 30,148' N	021° 05,105' W	401.2	
MSM85_81-1	CTD/ROS	2019-08-04 01:40	69° 34,758' N	021° 15,298' W	429.2	
MSM85_82-1	CTD/ROS	2019-08-04 02:48	69° 39,298' N	021° 25,535' W	463.9	
MSM85_83-1	CTD/ROS	2019-08-04 03:55	69° 43,876' N	021° 35,888' W	456.9	
MSM85_84-1	CTD/ROS	2019-08-04 05:02	69° 48,496' N	021° 46,140' W	439.2	
MSM85_85-1	CTD/ROS	2019-08-04 06:08	69° 53,082' N	021° 56,516' W	444.4	
MSM85_86-1	CTD/ROS	2019-08-04 07:04	69° 56,598' N	022° 05,090' W	441.5	
MSM85_87-1	CTD/ROS	2019-08-04 07:59	69° 59,991' N	022° 13,037' W	150.8	
MSM85_88-1	CTD/ROS	2019-08-04 09:43	70° 10,026' N	021° 45,594' W	424.4	
MSM85_89-1	CTD/ROS	2019-08-04 11:02	70° 14,990' N	021° 31,788' W	471.5	
MSM85_90-1	CTD/ROS	2019-08-04 12:12	70° 19,996' N	021° 17,881' W	427.3	
MSM85_40-1	Towfish	2019-08-04 15:37	70° 43,993' N	020° 22,151' W	273.7	on deck
MSM85_91-1	CTD/ROS	2019-08-04 22:17	71° 08,983' N	021° 36,255' W	81.4	
MSM85_92-1	CTD/ROS	2019-08-04 23:33	71° 08,841' N	021° 21,988' W	207.2	
MSM85_93-1	CTD/ROS	2019-08-05 01:56	71° 08,698' N	021° 02,892' W	247.4	
MSM85_94-1	CTD/ROS	2019-08-05 03:32	71° 08,461' N	020° 44,431' W	315.5	
MSM85_95-1	CTD/ROS	2019-08-05 04:39	71° 08,281' N	020° 25,990' W	379.5	
MSM85_96-1	CTD/ROS	2019-08-05 06:21	71° 08,104' N	020° 07,513' W	334.3	
MSM85_97-1	CTD/ROS	2019-08-05 07:24	71° 07,915' N	019° 49,026' W	352.2	
MSM85_98-1	CTD/ROS	2019-08-05 08:32	71° 07,746' N	019° 30,564' W	437.7	
MSM85_99-1	CTD/ROS	2019-08-05 09:28	71° 07,660' N	019° 21,275' W	460.3	
MSM85_100-1	CTD/ROS	2019-08-05 10:41	71° 07,529' N	019° 12,041' W	643.1	
MSM85_101-1	CTD/ROS	2019-08-05 12:26	71° 07,438' N	019° 02,781' W	953.7	
MSM85_102-1	CTD/ROS	2019-08-05 14:10	71° 07,320' N	018° 53,618' W	1237.4	
MSM85_103-1	CTD/ROS	2019-08-05 16:17	71° 07,212' N	018° 35,061' W	1559.6	
MSM85_104-1	CTD/ROS	2019-08-05 18:59	71° 07,032' N	018° 16,470' W	1675.5	
MSM85_105-1	Towfish	2019-08-05 20:17	71° 06,640' N	018° 13,905' W	1680.8	in the water
MSM85_106-1	CTD/ROS	2019-08-05 20:56	71° 06,831' N	017° 58,043' W	1695.6	
MSM85_107-1	CTD/ROS	2019-08-05 23:18	71° 06,422' N	017° 21,005' W	1683.3	
MSM85_108-1	CTD/ROS	2019-08-06 01:40	71° 06,126' N	016° 44,104' W	1300.7	
MSM85_109-1	CTD/ROS	2019-08-06 03:46	71° 05,788' N	016° 07,027' W	1848.9	
MSM85_110-1	CTD/ROS	2019-08-06 06:07	71° 05,383' N	015° 30,049' W	1047.7	
MSM85_111-1	CTD/ROS	2019-08-06 08:09	71° 04,984' N	014° 53,042' W	754.3	
MSM85_112-1	CTD/ROS	2019-08-06 10:03	71° 04,620' N	014° 16,058' W	975.5	
MSM85_113-1	CTD/ROS	2019-08-06 11:43	71° 04,378' N	013° 51,031' W	500.3	
MSM85_114-1	CTD/ROS	2019-08-06 13:00	71° 04,154' N	013° 26,007' W	808.1	

MSM85_115-1	CTD/ROS	2019-08-06 14:29	71° 03,931' N	013° 01,988' W	657.3	
MSM85_116-1	CTD/ROS	2019-08-06 17:57	71° 32,972' N	012° 10,059' W	2590.4	
MSM85_116-2	Float	2019-08-06 19:35	71° 33,010' N	012° 10,013' W	2594.4	WMO 7900537
MSM85_117-1	CTD/ROS	2019-08-06 21:02	71° 39,091' N	012° 54,043' W	1934.5	
MSM85_118-1	CTD/ROS	2019-08-06 23:32	71° 44,088' N	013° 30,052' W	1480.9	
MSM85_119-1	CTD/ROS	2019-08-07 01:44	71° 49,086' N	014° 05,996' W	1501.0	
MSM85_120-1	CTD/ROS	2019-08-07 03:55	71° 54,072' N	014° 42,048' W	1162.1	
MSM85_121-1	CTD/ROS	2019-08-07 05:56	71° 59,069' N	015° 18,020' W	1302.3	
MSM85_122-1	CTD/ROS	2019-08-07 07:58	72° 04,049' N	015° 54,059' W	1384.1	
MSM85_123-1	CTD/ROS	2019-08-07 10:09	72° 09,061' N	016° 30,031' W	1698.6	
MSM85_124-1	CTD/ROS	2019-08-07 12:29	72° 14,065' N	017° 06,047' W	1581.9	
MSM85_125-1	CTD/ROS	2019-08-07 14:14	72° 16,568' N	017° 24,034' W	1021.6	
MSM85_126-1	CTD/ROS	2019-08-07 15:22	72° 17,826' N	017° 33,003' W	908.2	
MSM85_127-1	CTD/ROS	2019-08-07 16:24	72° 18,628' N	017° 39,040' W	834.4	
MSM85_128-1	CTD/ROS	2019-08-07 17:48	72° 19,886' N	017° 48,047' W	703.9	
MSM85_129-1	CTD/ROS	2019-08-07 19:00	72° 21,563' N	018° 00,037' W	478.7	
MSM85_130-1	CTD/ROS	2019-08-07 20:07	72° 24,074' N	018° 17,939' W	242.0	
MSM85_131-1	CTD/ROS	2019-08-07 21:09	72° 26,583' N	018° 35,978' W	267.9	
MSM85_132-1	CTD/ROS	2019-08-07 22:25	72° 29,060' N	018° 53,898' W	259.6	
MSM85_105-1	Towfish	2019-08-07 22:47	72° 29,051' N	018° 53,931' W	261.0	on deck
MSM85_133-1	CTD/ROS	2019-08-08 00:28	72° 31,578' N	019° 12,074' W	249.9	
MSM85_134-1	CTD/ROS	2019-08-08 02:12	72° 34,051' N	019° 30,029' W	260.0	
MSM85_135-1	CTD/ROS	2019-08-08 03:22	72° 36,564' N	019° 47,975' W	233.0	
MSM85_136-1	CTD/ROS	2019-08-08 04:32	72° 39,067' N	020° 05,918' W	178.4	
MSM85_137-1	CTD/ROS	2019-08-08 05:50	72° 41,604' N	020° 24,435' W	222.5	
MSM85_138-1	CTD/ROS	2019-08-08 07:40	72° 44,070' N	020° 42,073' W	289.1	
MSM85_139-1	CTD/ROS	2019-08-08 09:23	72° 46,536' N	021° 00,040' W	313.3	
MSM85_140-1	CTD/ROS	2019-08-08 10:31	72° 48,911' N	021° 17,228' W	279.3	
MSM85_141-1	Towfish	2019-08-08 11:06	72° 50,037' N	021° 14,622' W	264.9	in the water
MSM85_141-1	Towfish	2019-08-08 12:57	73° 05,732' N	020° 32,590' W	161.6	on deck
MSM85_142-1	Towfish	2019-08-08 17:28	73° 28,004' N	019° 50,279' W	174.8	in the water
MSM85_143-1	CTD/ROS	2019-08-08 21:36	74° 10,989' N	019° 15,040' W	205.5	
MSM85_144-1	CTD/ROS	2019-08-08 22:46	74° 09,009' N	018° 55,076' W	259.6	
MSM85_142-1	Towfish	2019-08-08 23:32	74° 08,587' N	018° 49,684' W	255.4	on deck
MSM85_145-1	CTD/ROS	2019-08-09 00:41	74° 06,992' N	018° 34,917' W	228.4	
MSM85_146-1	CTD/ROS	2019-08-09 02:12	74° 04,978' N	018° 14,943' W	192.4	
MSM85_147-1	CTD/ROS	2019-08-09 03:47	74° 02,960' N	017° 55,044' W	174.2	
MSM85_148-1	CTD/ROS	2019-08-09 05:55	74° 01,014' N	017° 35,009' W	166.8	
MSM85_149-1	CTD/ROS	2019-08-09 08:25	73° 59,016' N	017° 14,809' W	172.7	
MSM85_150-1	CTD/ROS	2019-08-09 11:11	73° 56,944' N	016° 54,986' W	215.6	
MSM85_151-1	CTD/ROS	2019-08-09 13:33	73° 54,986' N	016° 35,089' W	229.9	
MSM85_152-1	CTD/ROS	2019-08-09 15:37	73° 52,973' N	016° 15,046' W	213.7	
MSM85_153-1	Towfish	2019-08-09 16:22	73° 51,452' N	015° 59,963' W	261.7	in the water
MSM85_154-1	CTD/ROS	2019-08-09 16:36	73° 50,991' N	015° 55,072' W	263.6	
MSM85_155-1	CTD/ROS	2019-08-09 17:43	73° 48,993' N	015° 35,069' W	789.0	
MSM85_156-1	CTD/ROS	2019-08-09 18:57	73° 46,993' N	015° 15,091' W	1314.9	
MSM85_157-1	CTD/ROS	2019-08-09 20:36	73° 44,986' N	014° 55,042' W	1732.0	
MSM85_158-1	CTD/ROS	2019-08-09 22:25	73° 42,977' N	014° 35,060' W	2056.0	
MSM85_159-1	CTD/ROS	2019-08-10 00:54	73° 38,999' N	013° 55,003' W	2419.9	
MSM85_160-1	CTD/ROS	2019-08-10 03:32	73° 34,991' N	013° 15,098' W	2616.2	
MSM85_161-1	CTD/ROS	2019-08-10 06:15	73° 30,989' N	012° 35,078' W	2741.5	
MSM85_162-1	CTD/ROS	2019-08-10 09:10	73° 27,010' N	011° 55,094' W	2793.6	
MSM85_163-1	Float	2019-08-10 10:54	73° 27,119' N	011° 53,933' W	2795.2	WMO 7900536
MSM85_164-1	Float	2019-08-10 20:26	75° 00,000' N	007° 38,288' W	3362.8	WMO 7900535
MSM85_153-1	Towfish	2019-08-11 06:49	76° 51,983' N	002° 59,562' W	1992.8	on deck
MSM85_165-1	CTD/ROS	2019-08-11 12:48	77° 29,989' N	003° 42,875' W	2937.9	no samples
MSM85_166-1	CTD/ROS	2019-08-11 19:12	77° 29,983' N	005° 02,395' W	1142.9	
MSM85_167-1	CTD/ROS	2019-08-11 21:04	77° 29,977' N	004° 52,465' W	1283.1	
MSM85_168-1	CTD/ROS	2019-08-11 23:02	77° 29,972' N	004° 38,722' W	1443.2	
MSM85_169-1	CTD/ROS	2019-08-12 01:12	77° 29,973' N	004° 24,732' W	1812.5	
MSM85_170-1	CTD/ROS	2019-08-12 03:31	77° 29,966' N	004° 10,748' W	2639.8	

7.2 Sample List

Table 7.2: Trace metal clean surface samples collected by the towed fish. Nut = Nutrients, DTM: dissolved trace metals, TDTM = Total dissolvable trace metals, Chl = Chlorophyll a, FCM = Flow cytometry, B_{12} = Vitamin B_{12}, POC/N = particulate organic carbon and nitrogen, DOC = dissolved oganic carbon, FDOM = colored dissolved organic matter (CDOM) and fluorescent dissolved organic matter (FDOM), TEP = coomassie stainable particles (csp) and transparent exopolymer particles (tep).

Sample ID	Stn	UTC date (dd/mm)	UTC time (hh:mm)	Nut	DTMs	TDTM	Chl	FCM	RNA/DNA/Prot	B_{12}	POC/N	DOC	FDOM	TEP
Fish 1	1-1	24/07	15:22	X	X	X	X	X	X	X	X	X	X	X
Fish 2	1-1	25/07	01:10	X	X	X								
Fish 3	1-1	25/07	09:30	X	X									
Fish 4	1-1	25/07	14:53	X	X	X	X	X	X	X	X	X	X	X
Fish 5	1-1	25/07	22:45	X	X									
Fish 6	1-1	26/07	09:10	X	X									
Fish 7	1-1	26/07	15:00	X	X	X	X	X	X	X	X	X	X	X
Fish 8	1-1	26/07	20:40	X	X									
Fish 9	1-1	27/07	07:15	X	X	X	X	X	X	X	X	X	X	X
Fish 10	1-1	27/07	09:23	X	X									
Fish 11	1-1	27/07	13:15	X	X									
Fish 12	1-1	27/07	20:15	X	X	X								
Fish 13	1-1	28/07	06:00	X	X									
Fish 14	1-1	28/07	12:00	X	X									
Fish 15	1-1	28/07	15:00	X	X	X	X	X	X	X	X	X	X	X
Fish 16	1-1	28/07	19:26	X	X		X							
Fish 17	1-1	28/07	22:50	X	X	X	X							
Fish 18	20-1	29/07	14:15	X	X	X	X	X	X	X	X	X	X	X
Fish 19	20-1	29/07	20:45	X	X		X							
Fish 20	20-1	30/07	04:08	X	X		X							
Fish 21	40-1	01/08	08:30	X	X	X	X							
Fish 22	40-1	01/08	14:30	X	X		X	X	X	X	X	X	X	X
Fish 23	40-1	01/08	22:10	X	X		X							
Fish 24	40-1	02/08	02:00	X	X		X	X	X	X	X	X	X	X
Fish 25	40-1	02/08	05:45	X	X		X							
Fish 26	40-1	02/08	08:45	X	X	X	X							
Fish 27	40-1	02/08	14:35	X	X		X							
Fish 28	40-1	02/08	19:20	X	X	X	X							
Fish 29	40-1	03/08	02:43	X	X									
Fish 30	40-1	03/08	08:25	X	X	X	X							
Fish 31	40-1	03/08	13:50	X	X	X	X	X	X	X	X	X	X	X
Fish 32	40-1	03/08	19:30	X	X		X							
Fish 33	40-1	03/08	23:23	X	X		X							
Fish 34	40-1	04/08	02:35	X	X	X	X							

Fish 35	40-1	04/08	07:40	X	X		X							
Fish 36	40-1	04/08	11:42	X	X		X							
Fish 37	40-1	04/08	13:10	X	X	X	X	X	X	X	X	X	X	X
Fish 38	40-1	04/08	15:05	X	X		X							
Fish 39	105-1	05/08	20:35	X	X	X	X							
Fish 40	105-1	05/08	23:00	X	X		X							
Fish 41	105-1	06/08	05:40	X	X	X	X							
Fish 42	105-1	06/08	11:05	X	X		X							
Fish 43	105-1	06/08	16:30	X	X	X	X	X	X	X	X	X	X	
Fish 44	105-1	06/08	17:48	X	X		X							
Fish 45	105-1	06/08	23:05	X	X		X							
Fish 46	105-1	07/08	05:15	X	X	X	X							
Fish 47	105-1	07/08	09:30	X	X		X							
Fish 48	105-1	07/08	12:15	X	X		X							
Fish 49	105-1	07/08	15:10	X	X	X	X							
Fish 50	105-1	07/08	18:38	X	X		X							
Fish 51	105-1	07/08	21:48	X	X		X							
Fish 52	141-1	08/08	11:30	X	X	X	X							
Fish 53	141-1	08/08	12:30	X	X	X	X	X	X	X	X	X	X	X
Fish 54	142-1	08/08	17:50	X	X		X							
Fish 55	142-1	08/08	20:50	X	X		X							
Fish 56	142-1	08/08	23:20	X	X	X	X							
Fish 57	153-1	09/08	17:25	X	X	X	X							
Fish 58	153-1	09/08	20:15	X	X		X							
Fish 59	153-1	09/08	22:10	X	X		X							
Fish 60	153-1	10/08	08:10	X	X	X	X							
Fish 61	153-1	10/08	12:45	X	X	X	X	X	X	X	X	X	X	X
Fish 62	153-1	10/08	15:30	X	X		X							
Fish 63	153-1	10/08	19:30	X	X		X							
Fish 64	153-1	10/08	23:40	X	X	X	X							
Fish 65	153-1	11/08	06:05	X	X		X							
Fish 66	171-1	12/08	08:25	X	X	X								

Table 7.3: Location of CTD samples obtained for Nutrients (Nut), RNA/DNA/Proteins, Vitamin B_{12} (B_{12}), flow cytometry (FCM) and Chlorophyll *a* (Chl).

Station	UTC Date	Latitude	Longitude	Nut	RNA/DNA /Proteins	B_{12}	FCM	Chl
10-1	27.07.19	62° 52,743' N	039° 15,794' W	X				
12-1	28.07.19	62° 33,250' N	038° 13,584' W	X				
14-1	28.07.19	62° 13,729' N	037° 11,413' W	X				
16-1	28.07.19	61° 54,231' N	036° 09,248' W	X				
19-1	29.07.19	61° 24,983' N	034° 35,982' W	X				
21-1	29.07.19	63° 49,971' N	031° 00,008' W	X				

24-1	30.07.19	64° 35,318' N	032° 02,507' W	X				
26-1	30.07.19	65° 00,016' N	032° 38,231' W	X				
28-1	30.07.19	65° 11,975' N	032° 54,858' W	X				
30-1	30.07.19	65° 20,975' N	033° 07,438' W	X				
31-1	31.07.19	65° 25,481' N	033° 13,821' W	X				
33-1	31.07.19	65° 40,002' N	033° 34,086' W	X				
35-1	31.07.19	65° 59,995' N	034° 02,040' W	X				
37-1	31.07.19	66° 09,982' N	034° 16,062' W	X				
38-1	31.07.19	66° 14,986' N	034° 23,098' W	X	X	X	X	X
41-1	01.08.19	68° 40,984' N	026° 17,526' W	X				
43-1	01.08.19	68° 36,740' N	026° 08,070' W	X				
46-1	01.08.19	68° 24,133' N	025° 40,201' W	X				
45-1	01.08.19	68° 28,323' N	025° 49,448' W	X				
48-1	01.08.19	68° 15,731' N	025° 21,679' W	X				
50-1	01.08.19	68° 09,519' N	025° 08,084' W	X				
52-1	01.08.19	68° 03,241' N	024° 54,353' W	X				
54-1	02.08.19	67° 50,558' N	024° 27,278' W	X				
58-1	02.08.19	67° 23,491' N	023° 40,378' W	X				
60-1	02.08.19	67° 11,079' N	023° 30,445' W	X				
63-1	02.08.19	66° 52,497' N	023° 17,019' W	X				
64-1	03.08.19	68° 12,004' N	018° 09,949' W	X				
66-1	03.08.19	68° 30,377' N	018° 51,144' W	X				
68-1	03.08.19	68° 48,685' N	019° 32,309' W	X				
70-1	03.08.19	68° 57,978' N	019° 52,937' W	X				
72-1	03.08.19	69° 07,078' N	020° 13,523' W	X				
75-1	03.08.19	69° 13,156' N	020° 27,127' W	X				
78-1	03.08.19	69° 20,913' N	020° 44,341' W	X				
81-1	04.08.19	69° 34,757' N	021° 15,300' W	X				
84-1	04.08.19	69° 48,494' N	021° 46,137' W	X				
87-1	04.08.19	69° 59,993' N	022° 13,024' W	X				
88-1	04.08.19	70° 10,027' N	021° 45,592' W	X				
89-1	04.08.19	70° 14,990' N	021° 31,789' W	X				
90-1	04.08.19	70° 19,998' N	021° 17,870' W	X				
91-1	04.08.19	71° 08,983' N	021° 36,254' W	X				
93-1	05.08.19	71° 08,699' N	021° 02,892' W	X				
95-1	05.08.19	71° 08,280' N	020° 25,990' W	X				
97-1	05.08.19	71° 07,913' N	019° 49,022' W	X				
99-1	05.08.19	71° 07,659' N	019° 21,278' W	X				
102-1	05.08.19	71° 07,321' N	018° 53,621' W	X				
104-1	05.08.19	71° 07,034' N	018° 16,470' W	X				
107-1	05.08.19	71° 06,422' N	017° 21,008' W	X				
109-1	06.08.19	71° 05,787' N	016° 07,030' W	X				
111-1	06.08.19	71° 04,983' N	014° 53,043' W	X				
114-1	06.08.19	71° 04,154' N	013° 26,007' W	X				
117-1	06.08.19	71° 39,092' N	012° 54,041' W	X				
120-1	07.08.19	71° 54,071' N	014° 42,048' W	X				

123-1	07.08.19	72° 09,061' N	016° 30,031' W	X				
125-1	07.08.19	72° 16,570' N	017° 24,040' W	X				
128-1	07.08.19	72° 19,886' N	017° 48,046' W	X				
132-1	07.08.19	72° 29,061' N	018° 53,899' W	X				
134-1	08.08.19	72° 34,054' N	019° 30,021' W	X				
136-1	08.08.19	72° 39,067' N	020° 05,915' W	X				
138-1	08.08.19	72° 44,070' N	020° 42,066' W	X				
140-1	08.08.19	72° 48,911' N	021° 17,225' W	X				
141-1	08.08.19	73° 05,732' N	020° 32,590' W	X				
143-1	08.08.19	74° 10,988' N	019° 15,040' W	X				
150-1	09.08.19	73° 56,948' N	016° 54,983' W	X				
154-1	09.08.19	73° 50,990' N	015° 55,068' W	X				
157-1	09.08.19	73° 44,985' N	014° 55,038' W	X				
159-1	10.08.19	73° 39,000' N	013° 55,009' W	X				
162-1	10.08.19	73° 27,054' N	011° 54,666' W	X				
166-1	11.08.19	77° 29,963' N	005° 02,223' W	X				
167-1	11.08.19	77° 29,999' N	004° 52,621' W	X	X	X	X	X
168-1	11.08.19	77° 29,973' N	004° 38,723' W	X				
170-1	12.08.19	77° 29,979' N	004° 10,760' W	X				

8 Data and Sample Storage and Availability

The raw and processed scientific data collected during MSM85 are stored in the data archives at University of Bremen and GEOMAR. They are available to all project partners and upon request to interested cooperating scientists. All scientific data will be submitted to PANGAEA (www.pangaea.de) within three years after the cruise, i.e. by August 2022.

Table 8.1 Overview of data availability

Data	Contact Person	Affiliation	Email
CTD/O_2, Multibeam Echosounder, Shipboard ADCP, lowered ADCP	Dr. Christian Mertens	Univ Bremen	cmertens@uni-bremen.de
SF6, CFC, Noble Gas Samples	Dr. Oliver Huhn	Univ Bremen	ohuhn@uni-bremen.de
Trace Gases	Dr. Damian L. Arévalo-Martínez	GEOMAR	darevalo@geomar.de
Nutrients, Trace Metals	Dr. Insa Rapp	GEOMAR	irapp@geomar.de
Organic Carbon	Dr. Mark Hopwood	GEOMAR	mhopwood@geomar.de

9 Acknowledgements

We thank Captain Ralf Schmidt and the entire crew of MARIA S. MERIAN for the friendly and cooperative atmosphere and their professional technical assistance. We are grateful to the Canadian, Icelandic, Norwegian, and Danish authorities for the permission to conduct scientific research in the respective exclusive economic zones. The Control Station German Research Vessels (Leitstelle Deutsche Forschungsschiffe), Klaus Bohn (LPL Projects + Logistics GmbH),

and Barbara Kozák (University of Bremen) provided logistical and administrative support. Financial support came from the German Ministry of Education and Research (BMBF) as part of the joint project *GROCE* (Greenland Ice Sheet – Ocean Interaction).

10 References

Arrigo, K.R., G. L. van Dijken, R. M. Castelao, H. Luo, Å. K. Rennermalm, M. Tedesco, T. L. Mote, H. Oliver, P. L. Yager, 2017. Melting glaciers stimulate large summer phytoplankton blooms in southwest Greenland waters, *Geophys. Res. Lett.*, 44(12), 6278–6285.

Bertrand, E. M., M. A. Saito, J. M. Rose, C. R. Riesselman, M. C. Lohan, A. E. Noble, P. A. Lee, G. R. DiTullio, 2007. Vitamin B_{12} and iron colimitation of phytoplankton growth in the Ross Sea, *Limnol. Oceanogr.*, 52(3), 1079-1093.

Bertrand, E. M. and A. E. Allen, 2012. Influence of vitamin B auxotrophy on nitrogen metabolism in eukaryotic phytoplankton, *Front. Microbiol.*, 3, 10.3389/fmicb.2012.00375.

Browning, T. J., E. P. Achterberg, I. Rapp, A. Engel, E. M. Bertrand, A. Tagliabue, C. M. Moore, 2017. Nutrient co-limitation at the boundary of an oceanic gyre, *Nature*, 551, 242-246.

Davey, M., G. A. Tarran, M. M. Mills, C. Ridame, R. J. Geider, J. LaRoche, 2008. Nutrient limitation of picophytoplankton photosynthesis and growth in the tropical North Atlantic, *Limnol. Oceanogr.*, 53(5), 1722–1733.

Hahm, D., C. F. Postlethwaite, K. Tamaki, and K. R. Kim, 2004. Mechanisms controlling the distribution of helium and neon in the Arctic seas: The case of the Knipovich Ridge, *Earth Planet. Sci. Lett.*, 229 (1), 125–139.

Hawkings, J. R., J. L. Wadham, M. Tranter, E. Lawson, A. Sole, T. Cowton, A. J. Tedstone, I. Bartholomew, P. Nienow, D. Chandler, J. Telling, 2015. The effect of warming climate on nutrient and solute export from the Greenland Ice Sheet, *Geochemi. Perspect. Lett.*, 1, 94–104.

Hopwood, M. J., D. Carroll, T. J. Browning, L. Meire, J. Mortensen, S. Krisch, E. P. Achterberg, 2018. Non-linear response of summertime marine productivity to increased meltwater discharge around Greenland, *Nat. Commun.*, 9(1), 3256.

Huhn, O., Hellmer, H.H., Rhein, M., Rodehacke, C., Roether, W., Schodlok, M.P., Schröder, M., 2008. Evidence of deep- and bottom-water formation in the western Weddell Sea. *Deep-Sea Res. II*, 55, (8-9), 1098–1116, doi:10.1016/j.dsr2.2007.12.015.

Huhn, O., T. Hattermann, P. E. D. Davis, E. Dunker, H. H. Hellmer, K. W. Nicholls, S. Østerhus, M. Rhein, M. Schröder, J. Sültenfuß, 2018. Basal melt and freezing rates from first noble gas samples beneath an ice shelf. *Geophys. Res. Lett.*, 45, doi:10.1029/2018GL079706.

Loose, B., Jenkins, W.J., 2014. The five stable noble gases are sensitive unambiguous tracers of glacial meltwater. *Geophys. Res. Lett.*, 41, (8), 2835-2841, doi: 10.1002/2013GL058804

Moore, C. M., M. M. Mills, K. R. Arrigo, I. Bergman-Frank, L. Bopp, P. W. Boyd, E. D. Galbraith, R. J. Geider, C. Guieu, S. L. Jaccard, T. D. Jickells, J. LaRoche, T. M. Lenton, N. M. Mahowald, E. Marañón, I. Marinow, J. K. Moore, T. Nakatsuka, A. Oschlies, M. A. Saito, T. F. Thingstad, A. Tsuda, O. Ulloa, 2013. Processes and patterns of oceanic nutrient limitation, *Nat Geosci*, 6.

Nielsdóttir, M. C., C. M. Moore, R. Sanders, D. J. Hinz, E. P. Achterberg, 2009. Iron limitation of the postbloom phytoplankton communities in the Iceland Basin, *Global Biogeochem. Cycles*, 23(3), doi: 10.1029/2008GB003410.

Rapp, I., C. Schlosser, D. Rusiecka, M. Gledhill, E. P. Achterberg, 2017. Automated preconcentration of Fe, Zn, Cu, Ni, Cd, Pb, Co, and Mn in seawater with analysis using high-resolution sector field inductively-coupled plasma mass spectrometry, *Analytica Chimica Acta,* 976, 1–13.

Rhein, M., R. Steinfeldt, O. Huhn, J. Sültenfuß, T. Breckenfelder, 2018. Greenland submarine melt water observed in the Labrador and Irminger Sea. *Geophys. Res. Lett.*, 45, 10,570-10,578, doi:10.1029/2018GL079110.

Ryan-Keogh, T. J., A. I. Macey, M. C. Nielsdóttir, M. I. Lucas, S. S. Steigenberger, M. C. Stinchcombe, E. P. Achterberg, T. S. Bibby, C. M. Moore, 2013. Spatial and temporal development of phytoplankton iron stress in relation to bloom dynamics in the high-latitude North Atlantic Ocean, *Limnol Oceanogr*, 58, 533–545.

Schlosser, P., 1986. Helium. A new tracer in Antarctic oceanography, *Nature*, 321, 233–235.

Sültenfuß, J., Roether, W., Rhein, M., 2009. The Bremen mass spectrometric facility for the measurement of helium isotopes, neon, and tritium in water. *Isotopes in Environmental and Health Studies,* 45 (2), 83–95, doi:10.1080/10256010902871929.